

2015-01-01

# Dynamic Triggering In The Coso Geothermal Field, 2004-2013

Richard A. Alfaro-Diaz

Follow this and additional works at: [https://digitalcommons.utep.edu/open\\_etd](https://digitalcommons.utep.edu/open_etd)



Part of the [Geology Commons](#), and the [Geophysics and Seismology Commons](#)

---

# DYNAMIC TRIGGERING IN THE COSO GEOTHERMAL FIELD, 2004-2013

RICHARD A. ALFARO-DIAZ

Department of Geological Sciences

APPROVED:

---

Aaron A. Velasco, Ph.D., Chair

---

Terry L. Pavlis, Ph.D.

---

Kristine M. Garza, Ph.D.

---

Charles Ambler, Ph.D.  
Dean of the Graduate School

Copyright ©

by

Richard A. Alfaro-Diaz

2015

# DYNAMIC TRIGGERING IN THE COSO GEOTHERMAL FIELD, 2004-2013

by

RICHARD A. ALFARO-DIAZ, B.S.

THESIS

Presented to the Faculty of the Graduate School of

The University of Texas at El Paso

in Partial Fulfillment

of the Requirements

for the Degree of

MASTER OF SCIENCE

Department of Geological Sciences

THE UNIVERSITY OF TEXAS AT EL PASO

May 2015



## **Acknowledgements**

This thesis would not have been possible without the guidance and help of several individuals, who in one way or another assisted in the preparation and completion of this research. First and Foremost, I would like to give special thanks to my advisor Dr. Aaron Velasco for his constant support, advice, and encouragement. I also thank Dr. Debi Kilb, Dr. Terry Pavlis, and Dr. Kristine Garza for reviewing this thesis and supporting my research.

This work was supported by the National Science Foundation under Grant Number EAR-1053376 and the GK-12 National Science Foundation Grant Number DGE-0947992.

## Abstract

We take advantage of EarthScope's USArray Transportable Array (TA), regional seismic networks to investigate 154  $M \geq 7$  earthquakes over a ten-year period (2004- 2013), in search of remotely triggered seismicity within the continental United States. We conduct an automated search to detect high frequency signals (which may indicate triggering of small local earthquakes) using a time window of 5 hours before and after each mainshock. The automated detection applies a short-term average (STA) to long-term-average (LTA) algorithms, to create a catalogue of detections. Using the catalog we search for an increase in detection rates after each main-shock. Sharp increases in detection rates may indicate triggered seismicity that is either instantaneous or delayed.

Here, we use both STA/LTA detection methods and local earthquake catalogs to investigate remote triggering in the Coso Geothermal Field (CGF); geothermal sites have long been suggested as areas susceptible to remote triggering of seismicity. Of 154 remote mainshocks ( $M \geq 7$ ) studied, we find 34 mainshocks (22%) likely triggered local seismicity in the CGF region as a result of an imposing transfer of dynamic stress from the remote mainshock events. We assume there is a triggered response in the CGF based on the increase in the magnitude and frequency (rate) from pre-mainshock to post-mainshock auto-detection rates and cataloged seismicity. We observe both instantaneous (16 events) and delayed (18 events) triggering of local seismicity within  $\pm 5$  hours of the mainshock. We suggest remote triggering in the CGF region is enhanced by the orientation (back-azimuth) of the passing seismic waves. We find several events align favorably with the local stress field and/or orientation of NNE-SSW trending faults in the CGF triggered region. We find triggering and non-triggering mainshocks (in terms of generated peak dynamic stresses and mainshock parameters) display similar

patterns. From this we surmise triggering in the CGF region to be strongly dependent on the state of regional stresses. We suggest that triggering is more likely to occur when critically stressed fault exists, this fault can respond to the passage of dynamic stresses in a manner triggering failure of the fault.

## Table of Contents

Acknowledgements .....	iv
Abstract .....	v
Table of Contents .....	vii
List of Tables .....	viii
List of Figures .....	ix
Introduction .....	1
Background .....	3
Data and Data Analysis .....	5
Applying STA/LTA detectors to 154 Mainshocks .....	10
Identification of Locally Triggered Seismicity .....	13
The Coso Geothermal Field a Regional Case Study .....	21
Coso Geothermal Field: Geology .....	21
Coso Geothermal Field: Data and Methods .....	24
Coso Geothermal Field: Triggering Mainshocks .....	31
Coso Geothermal Field: Mainshock Parameters .....	35
Discussion .....	39
Conclusion .....	46
References .....	48
Vita .....	52

## **List of Tables**

Table 1: Local seismicity near Coso Junction, CA.....	16
Table 2: Mainshock parameters all 154 mainshock events .....	26
Table 3: Parameters and Trigger Characteristics of Triggering Mainshocks .....	33

## List of Figures

Figure 1: Illustration of the process of Dynamic Triggering. ....	4
Figure 2: Locations of 154 $M \geq 7$ mainshock earthquakes (2004-2013). ....	6
Figure 3: Seismogram from Yellowstone swarm December 29, 2008. ....	8
Figure 4: Examination of the stacked cumulative number of Ev1 detections. ....	12
Figure 5: Seismic waveforms from the 27 February 2010 06:34:14 $M=8.8$ Offshore Bio Bio, Chile earthquake. ....	15
Figure 6: Regional location map of the Coso Range. ....	22
Figure 7: Tectonic map of the east flank of the Coso geothermal field. ....	23
Figure 8: Satellite image of the Coso Geothermal Field and surrounding region. ....	26
Figure 9: Map of locally triggered seismicity in the Coso geothermal field ....	32
Figure 10: World map of mainshock locations and focal mechanisms ....	37
Figure 11: Mainshock Parameters. ....	38
Figure 12: Instantaneous and Delayed Triggered Seismicity, originating from the Coso Geothermal Field. ....	43
Figure 13: Stress Map of Southern California, ....	45

## Introduction

Earthquakes occur on a frequent basis worldwide, yet linkages among events has remained an outstanding question. Large magnitude ( $M \geq 7$ ) events lead to devastating regional effects such as: ground shaking, subsidence, liquefaction, ground displacement and secondary effects such as tsunamis, flooding and fire. These events pose a direct danger to human life and infrastructure. These large earthquakes generate seismic wave energy that propagates through the Earth and can disturb the local stress field thousands of km away from the main-shock, and trigger seismicity.

Previous studies demonstrate that the passage of seismic waves originating from large Magnitude ( $M \geq 7$ ) earthquakes, can trigger seismicity (i.e. small earthquakes and tremor) at remote distances [e.g., *Velasco et al.*, 2008; *Guilhem et al.*, 2010; *Chao et al.*, 2012]. The disturbance leading to these triggered seismic events is typically interpreted as the product of propagating dynamic stresses produced by seismic waves. [*Hill et al.*, 1993; *Brodsky et al.*, 2000; *Kilb et al.*, 2000; *Gomberg et al.*, 2001, 2004; *West et al.*, 2005, *Parsons et al.*, 2012]. Large earthquakes produce surface waves that travel within the Earth's crust as elastic disturbances that distort and modify stress on fault planes that lie in their paths [*Parsons et al.*, 2012].

It is currently hypothesized that the main disturbance contributing to triggered seismic events is the passing of large amplitude surface waves of  $M \geq 7$  earthquakes [*Velasco et al.*, 2008; *Peng et al.*, 2009; *Peng et al.*, 2011]. Important factors that control the potential of triggering an earthquake include the amplitude of the passing surface waves and the back azimuth angles of the surface waves (both Love and Rayleigh waves) [*Chao et al.*, 2013]. Surface waves exhibit properties such as dispersion, geometric spreading and unique radiation patterns. Different periods of surface waves travel at different velocities and are therefore not

sharp arrivals as the wave energy is dispersed. Triggered seismic events can either occur instantaneously during the passage of seismic waves of mainshock or may be delayed [Gonzalez-Huizar *et al.*, 2012].

How one earthquake leads to another can impact our understanding and definition of seismic hazards in the continental United States. To address this we take advantage of resources such as the Incorporated Research Institutes for Seismology (IRIS) Data Management Center (DMC), we obtained seismograms using the Standing Order of Data (SOD) interface from USArray's transportable array (TA) stations and regional seismic networks within the continental United States for a ten-year period (2004-2013). This investigation focuses on analyzing a time window of 5 hours before and 5 hours after 154 ( $M \geq 7$ ) earthquakes, to detect high frequency signals that may indicate triggering of earthquakes within the continental United States. We search for instantaneous and delayed triggered seismic events, statistically significant changes in detection rates, and associations with existing catalogues. We find one region in particular, the Coso Geothermal Field, is susceptible to significant dynamic instantaneous and delayed triggering.



## Background

Earthquakes can be triggered by changes in static stress or dynamic stress [Velasco et al., 2008]. Triggering by static stresses only affect areas in the near- field (a few fault lengths away) of a main-shock rupture [Hill and Prejean, 2014]. Regions where static stresses are very small that show an increase in seismicity rates, after the associated main-shock, are assumed to be dynamically triggered. Dynamic stresses travel along the wavetrain of a main-shock and can influence the stress state and trigger earthquakes in the near field [Kilb et al., 2000] and regions thousands of km away from the main-shock [Velasco et al., 2008; Brodsky et al., 2000; Tibi et al., 2003]. Figure 1 depicts dynamic stress changes, primarily caused by surface waves that are assumed to be responsible in triggering distant aftershock.

Surface waves generate strain and previous studies of dynamic triggering have correlated individual surface wave components, Love and Rayleigh, with triggered seismicity [Hill, 2008; Gonzalez-Huizar and Velasco, 2011]. Triggered seismic events can either occur instantaneously during the passage of the seismic wavetrain of a main-shock or after a delayed period of time. The physical process involved in the dynamic triggering of earthquakes is still unclear, although several theories have been proposed. Hypotheses for triggering include induced fluid pressure changes [Brodsky and Prejean, 2005], deformation by seismic waves [Parsons, 2005], and coulomb stress changes (local discrete deformation) [Kilb et al., 2002; Hill, 2008]. It is likely that a combination of these processes take part in the remote triggering of earthquakes.

Dynamic triggering has been widely observed following the 1992 M=7.3 Landers, CA earthquake [Hill et al., 1993]. For example, the 2002 Denali earthquake [Gomberg et al., 2004; Husen et al., 2004; Husker and Brodsky, 2004; Moran et al., 2004; Pankow et al., 2004; Prejean et al., 2004], and the 2011 Tohoku earthquake [Chao et al., 2012; Gonzalez-Huizar et al., 2012].

Gomberg *et al.*, 2001 observed increased rates of seismicity in several localities in California following both the 1992 M=7.3 Landers and 1999 M=7.1 Hector Mine earthquake, as well as a delayed increase in rates of seismicity (delayed triggering) in Long Valley, a volcanic region in California.

Observations of recent increases in seismicity in the midwestern United States may be related to deep wastewater injection sites [van der Elts *et al.*, 2013]. Fluid injection sites are susceptible to triggering by small changes in stress induced by the passage of seismic waves of distant large earthquakes. Most triggered injection sites have a long delay between the beginning of fluid injection and the start of seismicity, suggesting fluid injection can push a fault system into a critical state [van der Elts *et al.*, 2013]. Three sites: Prague, Oklahoma; Snyder, Texas; and Trinidad, Colorado hosted triggered events after large magnitude distant earthquakes: the Maule, Chile February 27 2010 M=8.8; Tohoku-oki March 11 2011 M=9.1; and Sumatra April 12 2012 M=8.6 [van der Elts *et al.*, 2013].

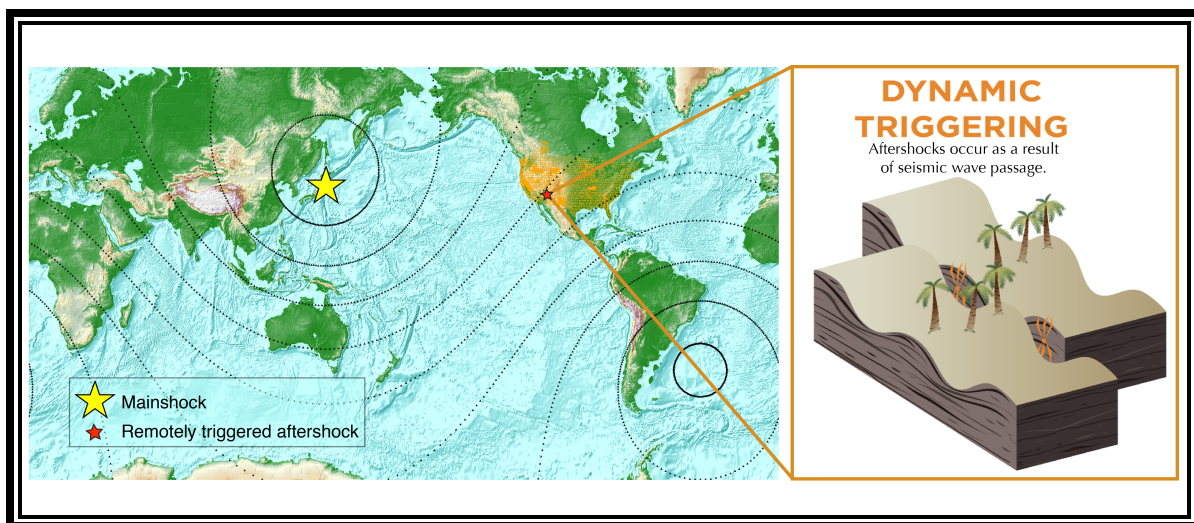


Figure 1: Illustration of the process of Dynamic Triggering of remote aftershocks. Taken from Velasco *et al.* (2015).

## Data and Data Analysis

We have obtained broadband 3-component data for the +450 stations in the USArray TA network and available regional seismic networks within the continental United States. The seismograms were obtained from Incorporated Research Institutes for Seismology (IRIS) Data Management Center (DMC) using the Standing Order of Data (SOD) interface for a ten-year period (2004-2013). This investigation focuses on analyzing a time window of 5 hours before and after 154  $M \geq 7$  earthquakes (2004-2013) (Figure 2). We search for dynamically triggered earthquakes, aiming to identify significant increases in the rate of seismicity in the continental United States following the mainshock earthquake. To prepare data for analysis, we use the Antelope software package provided by Boulder Real Time Technologies, Inc (BRTT). We create an Antelope database for all seismogram data acquired by SOD, and perform automated detections on waveforms, as described below.

We conduct an automated search to identify and detect high frequency signals on 3-component station data. Our detection algorithms implement a time domain short-term average (STA) to long-term-average (LTA) ratio to identify signals above the noise level and create a catalog of detections (which may or may not indicate an earthquake). We use four STA/LTA algorithms (e.g., 1s/10s; 4 s/40 s; 8 s/80 s; 16 s/160s) [Velasco *et. al*, 2015], seeking to identify un-cataloged, locally recorded small earthquakes on a single station within continuous seismic data.

We first acquire seismogram data from  $\pm 5$  hours of each main-shock event, generate and an Antelope database, high pass filter (5 Hz) the seismograms, and apply the automated STA/LTA algorithm for signal detections at each station recorded on three components. To remove any spurious detections we assume that a detection is real only if it was recorded on a

minimum of two channels (Figure 3). We statistically analyze results by comparing the seismicity rate 5-hours before and 5-hours after the main-shock event to identify an increase in seismicity rates (Figure 4) and to assess the potential for instantaneous and delayed triggering. Our preferred STA/LTA method of 4s/40s (STA/LTA) in combination with a requirement that assumes all real detections must be recorded on at least 2 channels at a single station effectively identifies small-triggered earthquakes [Velasco *et. al*, 2015].

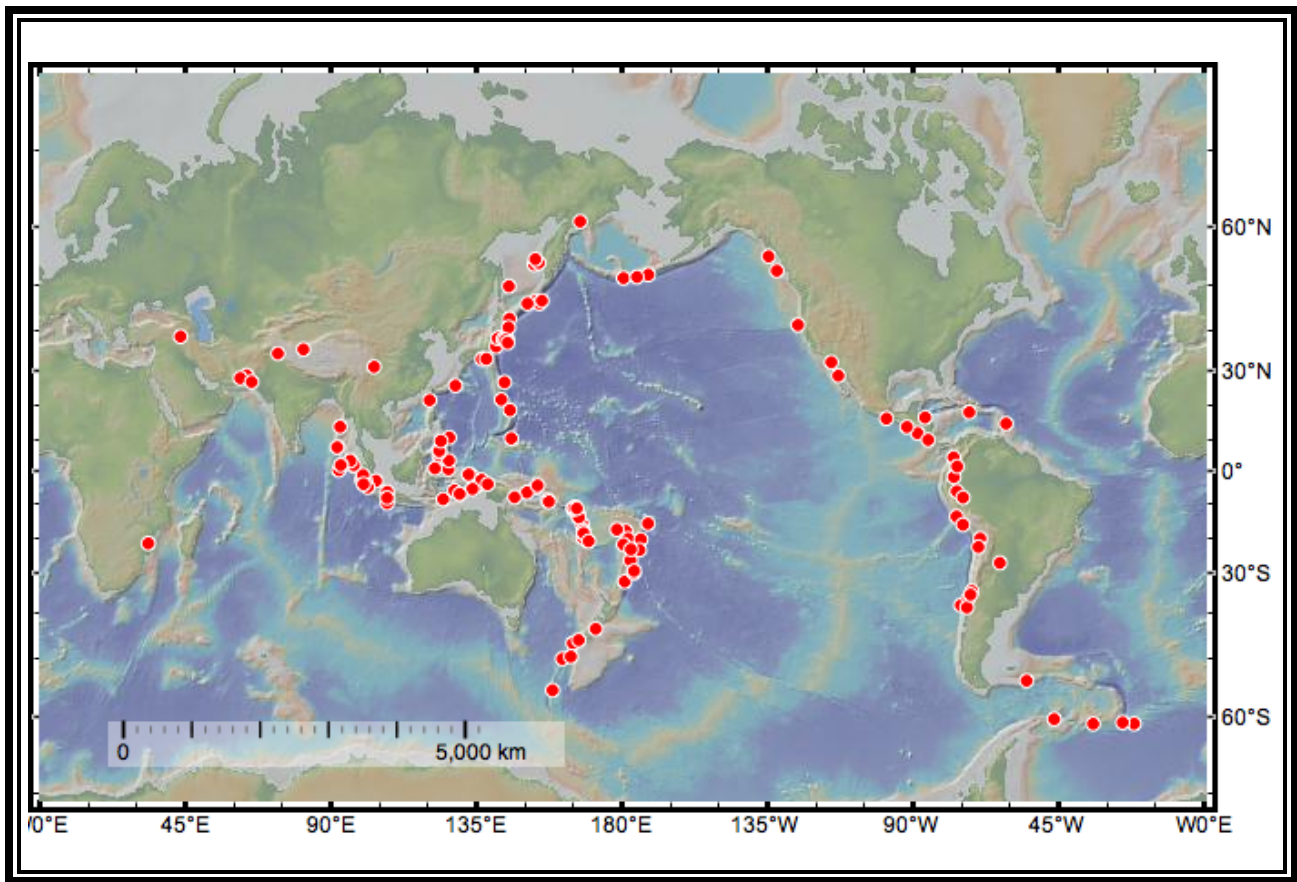
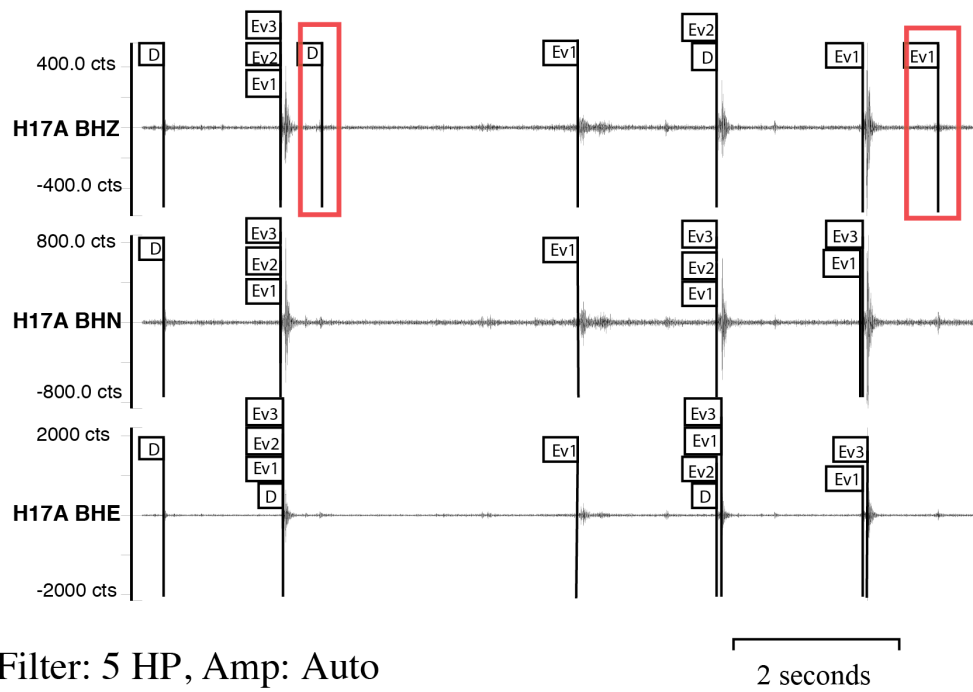


Figure 2: World map. Mercator projection, red circles indicated the locations of 154  $M \geq 7$  mainshock earthquakes (2004-2013) in our study. We apply an automated detection algorithm to  $\pm 5$  hours of the mainshock origin times, to find dynamically triggered seismicity in the continental United States.

### A) Seperate detections on each component



### B) Detections required to exist on two-components

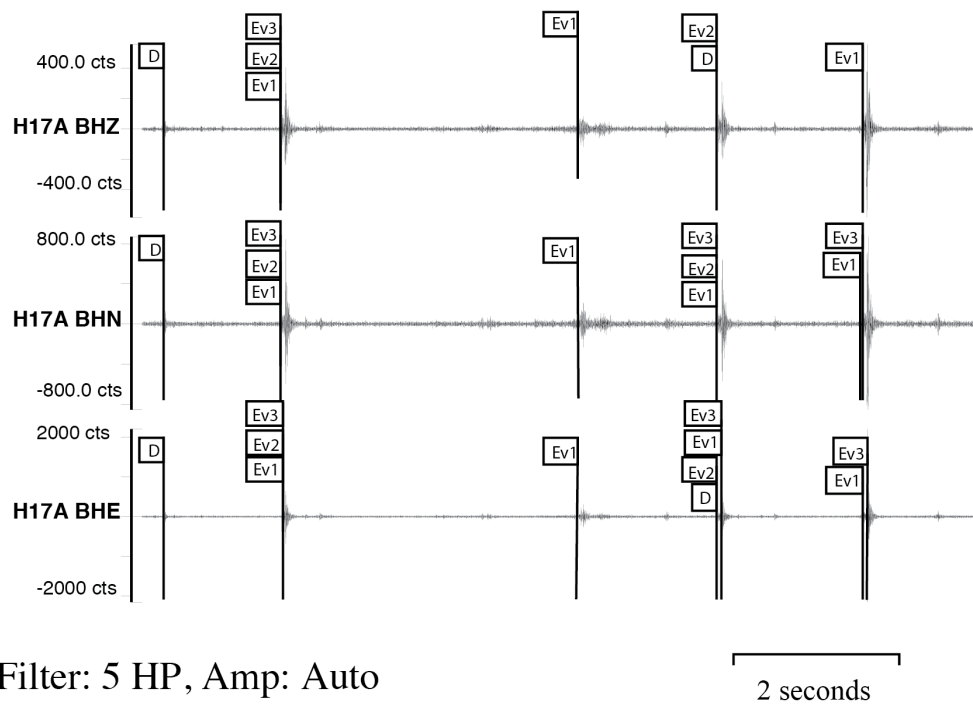


Figure 3: Seismogram from Yellowstone swarm December 29, 2008, recorded at station H17A. Vertical Black lines indicate STA/LTA algorithm detections with flags corresponding to ratios  $D=1$  s/10 s;  $Ev1=4$  s/40 s;  $Ev2=8$  s/80 s;  $Ev3=16$  s/160 s. (A) Initial detections derived from processing each channel individually (BHZ, BHN, BHE for vertical, horizontal North-South and horizontal east-west, respectively). (B) Detections that remain after removal of detections that were identified on only one component (i.e., we require a detection recorded on a minimum of two channels). In this example the first D-detected event is a false positive,  $Ev2$  does not detect the last earthquake in the waveform and there is one event (mid-trace) that is only successfully detected by  $Ev1$ . Taken from Velasco et al. (2015).

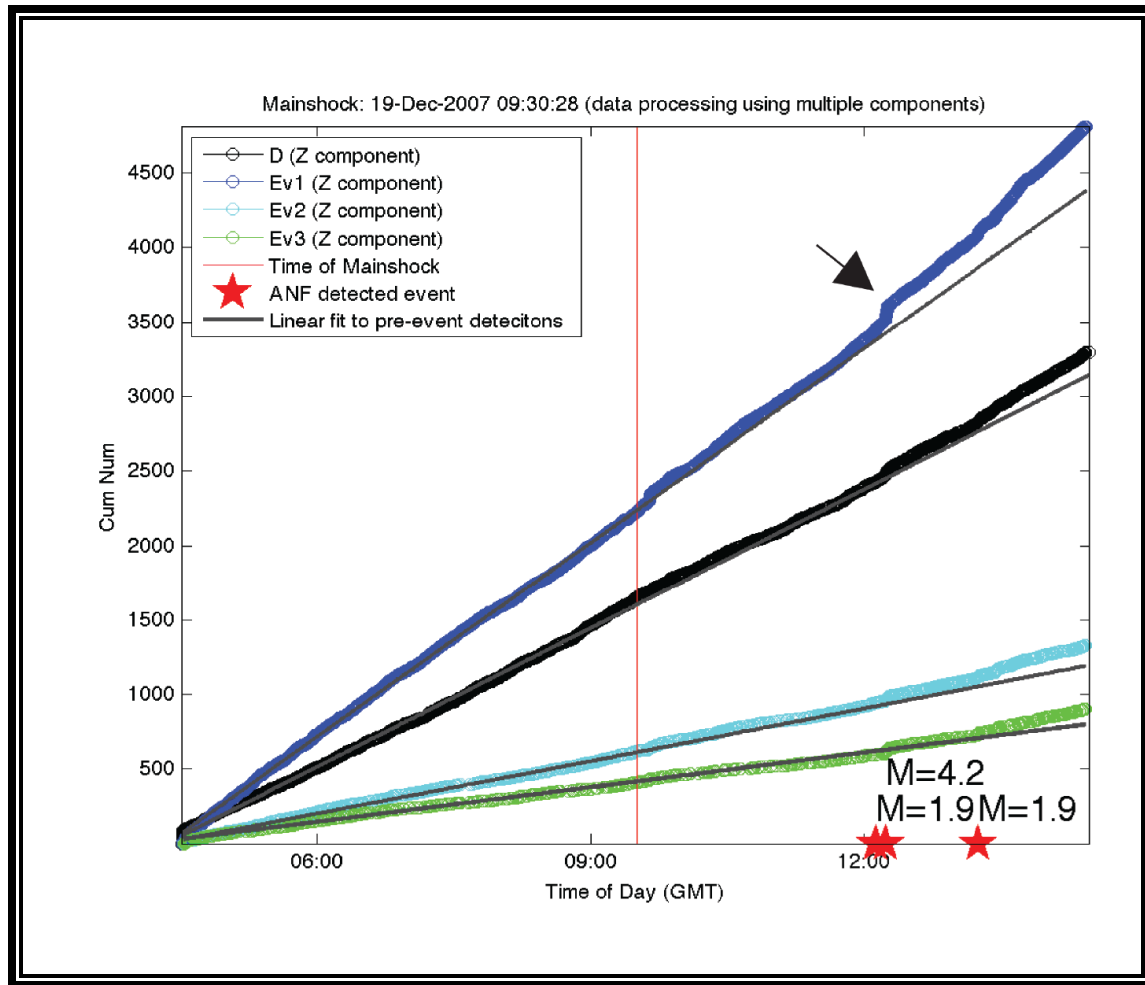


Figure 4: Cumulative number of detections plotted against time of day for the December 19, 2007 South Fiji Islands magnitude 7.8 earthquake. Automated time domain detections (D black; EV1 blue; Ev2 cyan; Ev3 green) corresponding to detection algorithms  $D = 1 \text{ s}/10 \text{ s}$ ;  $Ev1 = 4 \text{ s}/40 \text{ s}$ ;  $Ev2 = 8 \text{ s}/80 \text{ s}$ ;  $Ev3 = 16 \text{ s}/160 \text{ s}$ . Seismic stations within the continental United States, December 19, 2007 are used. Red stars correspond to events in then Array Network Facility (ANF) catalog, where the earthquake magnitude is listed above each star. Black arrow indicates a kink in detection where Ev1 (4 s /40 s) detections successfully at identify a real earthquake that corresponds to the ANF catalogue.

## **Applying STA/LTA detectors to 154 Mainshocks**

We apply four STA/LTA detectors (Velasco et al., 2015) to  $\pm 5$  hours from the mainshock origin time for 154  $M \geq 7$  earthquakes (2004-2013) (Figure 2) recorded by USArray. We assign the mainshock origin to time zero, stack the results from all 154 earthquakes at all stations, and count the number of detections at each station. We then color code detections by day and night, defining night as between 9PM-5AM local time and daytime 5AM-9PM local time. We find that for 76 events there appears to be a strong increase in the number of detections following the mainshock, 49 events have a strong decrease in the number of detections following the mainshock, and 29 showed no change in detection rate following the mainshock (Figure 4). A decrease is counter to what we expected. If anything, we expected either no change in the number of detections (i.e., lack of remote triggering) or a slight increase in the number of detections (i.e., potentially elevated seismicity caused by remotely triggered small earthquakes). As noted in Velasco et al. (2015), an increase or decrease in the detection rates (for the four STA/LTA detectors) may reflect anthropogenic noise. An increase may relate to the onset of daytime hours and a decreased rate of detections at the onset of nighttime hours. We find detection rates can indicate triggering in several cases when seismicity is prominent (Figure 4), although when waveforms are lacking seismic signals the STA/LTA detectors are prone to flag anthropogenic noise (Velasco et al., 2015). We discuss a successful identification of locally triggered seismicity using the Ev1 detection algorithm below.



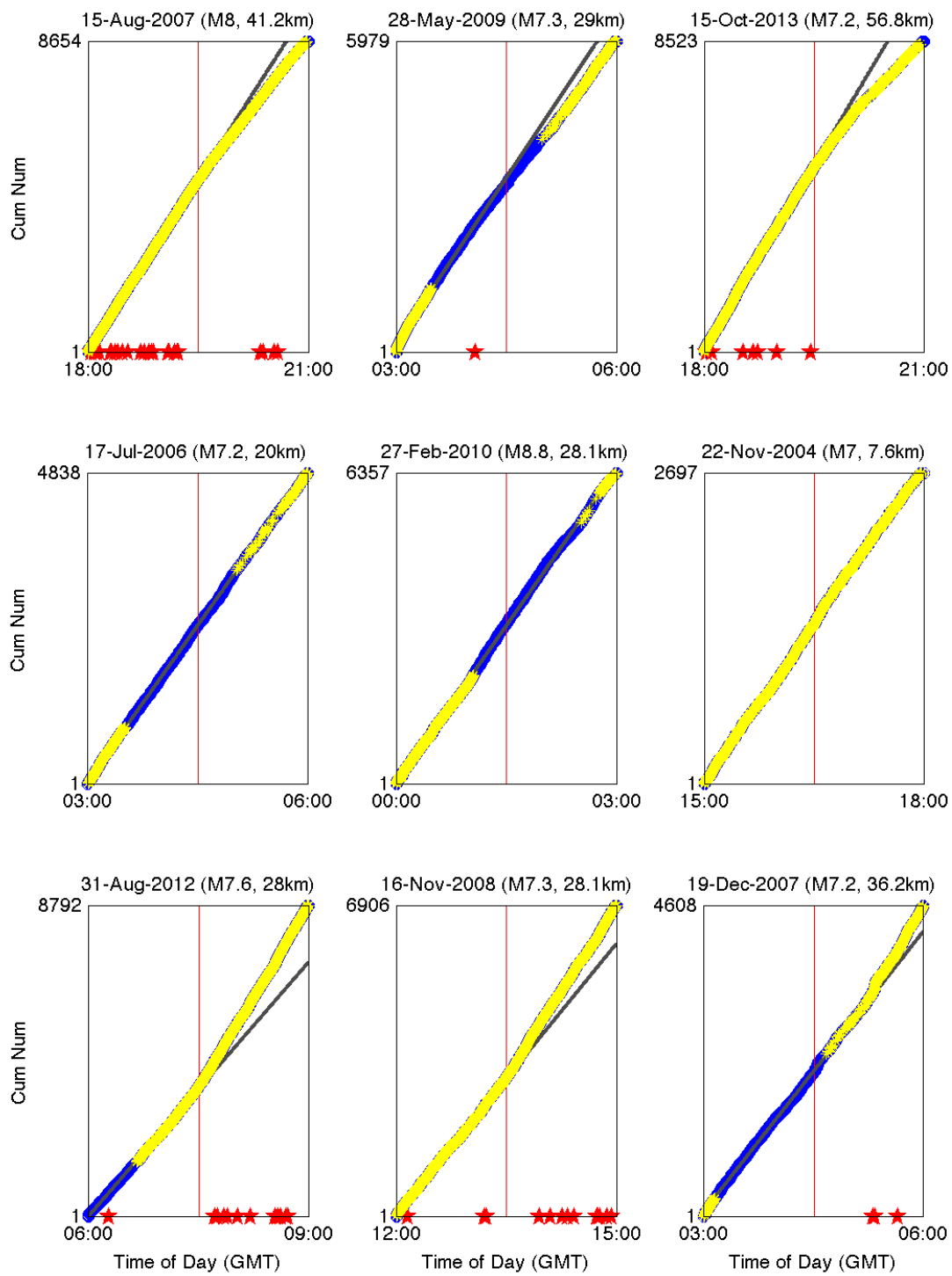


Figure 4: Examination of the stacked cumulative number of Ev1 detections as a function of time.

We evaluate data within  $\pm 5$  hours of the mainshock origin time, which is set to time zero. A linear fit to the pre-mainshock detections (grey line). The events can be categorized as: (top row) showing a decrease in the number of detections following the mainshock; (middle row) showing no change in the number of detections or (bottom row) showing a increase in the number of detections. The detections colored in yellow indicate a daytime detection.

## **Identification of Locally Triggered Seismicity, Applying the Ev1 detection method to the Feb. 27, 2010 Offshore Bio-Bio (M=8.8) Chile earthquake**

We apply the Ev1 detector to  $\pm 5$  hours of USArray data with respect to the Feb. 27, 2010 Offshore Bio-Bio (M=8.8) Chile earthquake. This mainshock event occurred at 06:34:14 UTC, which at the centroid of the USArray network in Denver, Colorado, was 11:34:14 PM MST. The fact that these data were collected during nighttime hours at the recording site is optimal, as nighttime hours have much less anthropogenic noise (Astiz et al., 2014; Velasco et al., 2015). For this 2010 mainshock event, the Ev1 detector net a total of 6166 detections, of which 2971 (48%) occurred within the 5 hours following the mainshock. This result indicates no strong change in earthquake rate for these stacked data. However, if we repeat this exercise using data from each individual station separately, we find evidence of a rate increase following the mainshock. At station R11A, a high signal-to-noise station, we find evidence of three regional earthquakes during the mainshock coda (Figure 5). The first of these occurred at the time of the mainshock's S-wave passage and the largest of the three events occurred at the time of the Love wave, while the other, and smallest event, occurred between the mainshock's S-wave and Love-wave arrivals (Figure 5). The  $Lg$ - minus  $P$ -wave arrival times for all three small quakes ( $\sim 38$  sec) indicates these events are several hundred km from station R11A.

One location that is consistent with the 330 km distance from station R11A is Coso Junction, CA (longitude= $-115.6^\circ$ ; Latitude= $38.35^\circ$ ). Based on the Southern California Seismic Network catalog, we determined the Coso region ( $33.5 \leq \text{Latitude} \leq 36.5$ ;  $-119 \leq \text{Longitude} \leq -117$ ) has a magnitude of completeness threshold of about magnitude one. Limiting the catalog to only events at or about magnitude one, we find that within a week-prior and a week-after the passage of seismic waves from the Chile mainshock the our Coso, CA, region catalog contains

23 ( $1 \leq M_L \leq 2.8$ ) and 66 events ( $1 \leq M_L \leq 3.8$ ), respectively (Table 1). Specifically we find an increase in seismic activity near Coso began after the passage of the *S*-wave (Figure 5) [Peng *et al.*, 2010a]. This increase in seismic activity suggests these events may constitute remote aftershocks from the M8.8 Chile earthquake triggered in the Coso Geothermal field, where in this case the onset of triggering began with the *S*-wave.

As a second test, to investigate if this increase in seismic activity in the Coso region is out of the norm, we examine the 1373 earthquakes in the region that occurred in the year 2010, which are at or above the magnitude of completeness level ( $M_L \geq 1$ ). On average this equates to about 4 earthquakes a day (1 every 6 hours), or about 28 earthquakes a week. This expected 28 events per-week value is on-par with the 23 events observed in the week prior to the Chile mainshock, but the 66 events in the week following the mainshock are a factor of three higher.

We know that the Coso region is subject to bursts of seismic activity, so we conduct a third test that uses the time separation between consecutive events. For the full catalog of 1373 events in the year 2010 catalog, the median time between consecutive events is 2.88 hours. Whereas for the 66 events in the week after the mainshock the median time between consecutive events is 1.08 hour, a factor of almost three smaller. Taken together these three tests suggest that the increase in seismic events in the week following the passage of the seismic waves from the Chile M8.8 mainshock is elevated in comparison with the typical background seismicity for the year 2010 near Coso Junction, CA by examining both the Southern California Seismic Network (SCSN) earthquake catalog and continuous waveform recordings. Finding the Ev1 method successfully identifies dynamically triggered seismicity corresponding to the Coso Geothermal Field, we focus our study specifically on Coso region to investigate the behavior of the site over 2004-2013.

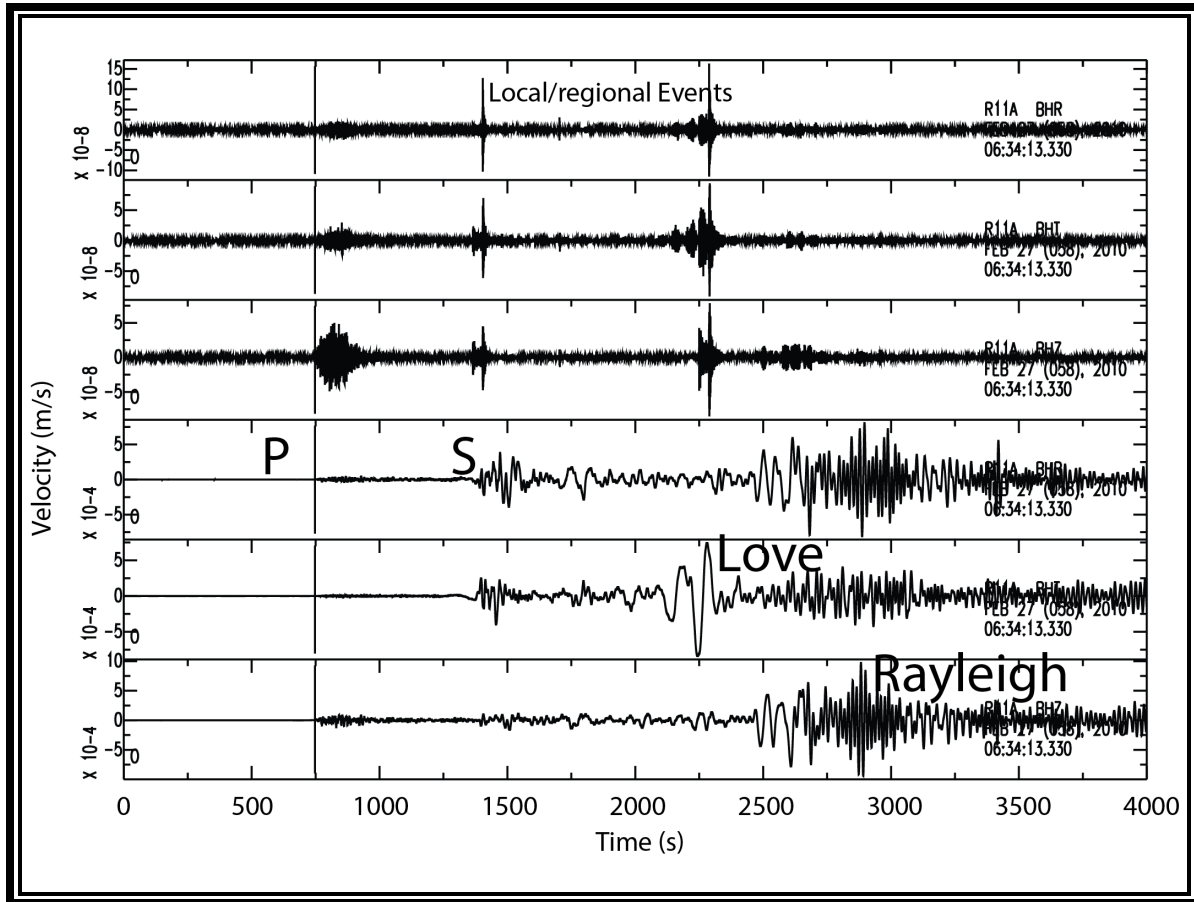


Figure 5: Seismic waveforms from the 27 February 2010 06:34:14 M=8.8 Offshore Bio Bio, Chile earthquake recorded at USArray TA station R11A. Top three waveforms are High pass at 5Hz, which removes the surface wave signal and reveals three regional events in the mainshock coda wave that arrive at the time of the S-wave (first event) the Love-wave (third and largest event) and at a time in between the S- and Love wave (second and smallest event). Bottom three waveforms display the raw waveform data. Taken from Velasco et al. (2015).

Table 1: Events near Coso Junction, CA ( $33.5 \leq \text{Latitude} \leq 36.5$ ;  $-119 \leq \text{Longitude} \leq -117$ ), which occurred within  $\pm 1$  week of the 27 February 2010 Chile earthquake (thicker line demarks the transition from before the mainshock to after the mainshock). These earthquakes range in magnitude from the completeness threshold of magnitude 1.0 up to a magnitude 3.8 event. Of these, there are only 5 events at or above magnitude 2 (none of which are above magnitude 3) in the week prior, to the mainshock whereas 23 events at or above magnitude 2 (6 of which are above magnitude 3) in the week after the mainshock.

ID	Magnitude	Date	Time	Latitude	Longitude	Depth (km)
10546173	1.51	2010/02/22	21:42:37	35.9380	-117.6400	3.90
10546189	2.50	2010/02/22	21:55:31	35.7530	-118.9990	21.30
10546285	1.73	2010/02/23	03:49:36	35.9240	-117.2750	6.80
10546757	2.33	2010/02/24	00:30:19	36.0640	-117.8670	4.50
10546885	1.03	2010/02/24	04:15:30	35.9550	-117.6530	3.10
10547061	1.28	2010/02/24	11:40:08	36.1150	-117.6590	5.40
10547109	1.13	2010/02/24	14:57:48	36.0570	-117.8820	5.90
10547221	1.10	2010/02/24	22:09:42	36.0550	-117.8510	5.10
10547261	1.11	2010/02/25	00:34:27	36.0690	-117.8590	0.70
10547309	1.53	2010/02/25	03:18:06	36.1060	-117.7160	2.40
10547365	1.03	2010/02/25	09:53:12	35.9750	-117.6480	3.30
14594612	1.42	2010/02/26	02:55:32	35.9310	-117.2870	4.90
14594620	1.45	2010/02/26	03:43:09	36.0390	-117.8370	0.00
14594628	1.40	2010/02/26	04:43:32	36.0680	-117.8440	2.70
14594692	1.18	2010/02/26	10:11:47	36.0630	-117.8730	1.80

14594708	2.64	2010/02/26	12:46:43	36.0630	-117.8710	2.80
14594716	1.63	2010/02/26	13:03:22	36.0630	-117.8770	2.70
14594724	2.69	2010/02/26	13:22:53	36.0730	-117.8800	2.90
14594860	2.79	2010/02/26	20:12:05	36.0640	-117.8720	2.80
28253759	1.06	2010/02/27	01:25:05	35.9310	-117.2640	6.40
14594900	1.78	2010/02/27	01:25:17	35.9320	-117.2590	6.20
14594924	1.14	2010/02/27	02:45:31	36.0650	-117.8670	4.60
14594956	1.79	2010/02/27	04:52:16	36.0700	-117.8710	4.40
<b>LINE</b>	<b>LINE</b>	<b>LINE</b>	<b>LINE</b>	<b>LINE</b>	<b>LINE</b>	<b>LINE</b>
14594996	2.91	2010/02/27	06:56:03	36.0730	-117.8780	2.50
14595004	2.10	2010/02/27	07:01:03	36.0710	-117.8820	1.50
14595012	3.45	2010/02/27	07:10:48	36.0620	-117.8880	0.60
14595020	2.26	2010/02/27	07:21:55	36.0690	-117.8880	2.00
14595076	1.52	2010/02/27	09:34:55	36.0670	-117.8830	1.30
14595140	1.35	2010/02/27	11:59:15	36.0670	-117.8810	3.70
14595156	1.56	2010/02/27	13:54:16	36.0710	-117.8690	4.60
14595164	3.11	2010/02/27	13:56:39	36.0660	-117.8830	2.00
14595172	3.30	2010/02/27	15:01:36	36.0610	-117.8770	2.60
14595180	1.26	2010/02/27	15:19:22	36.0690	-117.8630	4.50
14595196	1.29	2010/02/27	15:57:26	36.0640	-117.8700	3.90
14595236	1.13	2010/02/27	18:59:31	36.0760	-117.8700	4.00
14595244	1.47	2010/02/27	19:08:07	36.0590	-117.8820	2.50

14595276	1.47	2010/02/27	19:56:40	36.0620	-117.8760	2.70
14595284	1.09	2010/02/27	20:12:48	36.0560	-117.9070	5.70
14595292	2.80	2010/02/27	20:23:54	36.0630	-117.8890	0.10
14595316	1.82	2010/02/27	23:25:46	36.0610	-117.8760	2.60
14595380	1.76	2010/02/28	02:26:15	36.0690	-117.8650	4.30
14595452	3.43	2010/02/28	06:30:17	36.0600	-117.8820	0.90
28213759	2.60	2010/02/28	06:30:41	36.0600	-117.8780	1.10
14595460	1.76	2010/02/28	06:38:04	36.0710	-117.8710	4.10
14595468	3.13	2010/02/28	06:56:29	36.0610	-117.8790	2.70
14595476	2.58	2010/02/28	07:08:48	36.0620	-117.8790	2.40
14595556	1.48	2010/02/28	14:22:33	36.0680	-117.8600	4.80
14595580	1.49	2010/02/28	15:59:36	36.0660	-117.8730	4.10
14595628	1.26	2010/02/28	22:30:28	36.0600	-117.8740	2.90
14595676	1.54	2010/03/01	00:23:23	35.8050	-118.5370	5.50
14595684	1.13	2010/03/01	01:04:20	36.0390	-117.8190	1.30
14595708	1.67	2010/03/01	02:20:37	36.0640	-117.8700	3.00
14595756	1.27	2010/03/01	04:46:10	36.0630	-117.8720	2.80
14595764	1.46	2010/03/01	05:03:24	36.1000	-117.7980	7.90
14595820	3.76	2010/03/01	09:06:03	36.0700	-117.8790	0.90
14595828	2.10	2010/03/01	09:16:04	36.0690	-117.8710	2.20
14595844	1.93	2010/03/01	09:24:06	36.0660	-117.8680	2.70
14595852	1.21	2010/03/01	09:29:57	36.0650	-117.8670	4.30



14595868	2.75	2010/03/01	10:32:08	36.0640	-117.8700	2.20
14595876	2.61	2010/03/01	10:39:40	36.0650	-117.8760	2.50
10144402	2.75	2010/03/01	10:40:00	36.0650	-117.8820	1.90
14595884	1.20	2010/03/01	10:46:49	36.0700	-117.8850	2.20
14595892	2.31	2010/03/01	10:50:57	36.0690	-117.8750	0.60
14595916	2.11	2010/03/01	12:36:38	36.0690	-117.8810	2.40
14595964	1.15	2010/03/01	16:29:00	35.9510	-117.6290	4.40
10144566	1.44	2010/03/01	16:29:16	36.0920	-117.8660	0.00
14596172	1.00	2010/03/02	05:31:10	36.0530	-117.8720	5.20
14596196	1.47	2010/03/02	06:57:33	36.0660	-117.8690	3.50
14596204	3.47	2010/03/02	07:22:54	36.0650	-117.8730	2.50
10144482	2.20	2010/03/02	07:23:28	36.0630	-117.8600	3.40
14596212	1.86	2010/03/02	07:26:16	36.0660	-117.8810	2.10
14596228	1.39	2010/03/02	07:48:53	36.0610	-117.8730	2.40
14596252	1.06	2010/03/02	08:20:27	36.0600	-117.8660	5.00
14596260	1.21	2010/03/02	08:30:22	36.0580	-117.8700	4.70
14596308	1.73	2010/03/02	14:39:00	36.0640	-117.8730	3.00
14596340	1.06	2010/03/02	17:58:25	36.0620	-117.8660	4.90
14596388	1.61	2010/03/02	20:42:46	35.9830	-117.3250	6.10
14596420	1.01	2010/03/03	01:15:57	36.0650	-117.8780	0.70
14596508	1.22	2010/03/03	07:07:41	36.0590	-117.8800	2.50
14596564	1.68	2010/03/03	12:08:36	36.3220	-117.9200	8.30

14596796	1.24	2010/03/04	04:32:03	35.6380	-118.3930	8.80
14596924	1.08	2010/03/04	18:32:23	36.0720	-117.8530	4.20
14596972	1.49	2010/03/04	23:45:46	35.6830	-118.2000	11.20
14596988	1.08	2010/03/05	02:35:58	36.0700	-117.8740	4.50
14597012	2.94	2010/03/05	03:46:25	36.1380	-117.8390	1.10
14597044	1.19	2010/03/05	08:39:02	36.1400	-117.8430	5.60
14597060	1.07	2010/03/05	09:04:43	36.0550	-117.8440	4.90
14597092	2.09	2010/03/05	11:43:22	35.7120	-117.6330	12.90
14597372	1.09	2010/03/06	05:31:35	36.0940	-117.8440	1.60

## The Coso Geothermal Field a Regional Case Study

### COSO GEOTHERMAL FIELD: GEOLOGY

The Coso Geothermal Field (CGF) is located to east of the Sierra Nevada between Owens Valley and the Garlock fault in southern California within the present-day Basin and Range province (Figure 6). The CGF, situated above a shallow heat source (presumed to be a partially molten magma body) and is one of the most seismically active regions in the continental United States. The CGF is a highly-fractured, trans-tensional region [Davatzes and Hickman, 2006] affected by to both strike-slip and normal faulting. Faults within the CGF can be divided into two groups: 1) WNW striking dextral strike slip faults and minor NE trending faults sinistral strike-slip [Duffield *et al.*, 1980; Roquemore, 1984] that are relatively inactive by [Davatzes and Hickman, 2006] and 2) N to NNE striking normal faults that dip both west and east (Figure 7). According to Davatzes and Hickman (2006) the most prominent of these fault systems in the CGF is the Coso Wash normal fault which coincides with the eastern margin of the geothermal field. The Coso Wash fault is composed of several *en-echelon* NNE- SSW trending segments variably connected by NW- trending faults [Davatzes and Hickman, 2006]. Based on previous studies of geomorphic expression, offset hydrothermal deposits and basalt flow Davatzes and Hickman (2006) interpret these faults to be actively slipping.

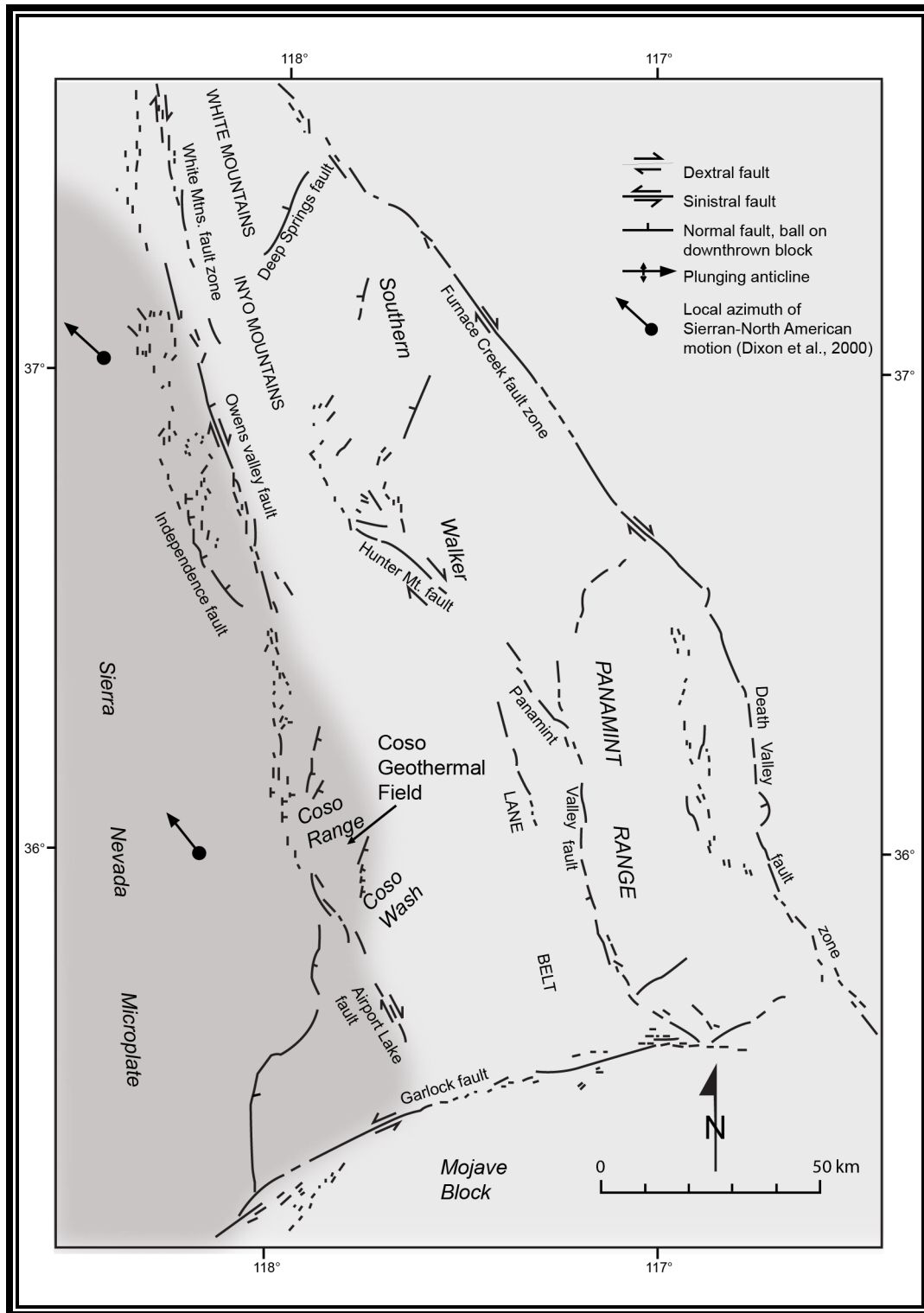


Figure 6: Regional location map of the Coso Range and the southern Walker Lane belt. Dark shading indicates the extent of the rigid Sierra Nevada microplate. Note that there is a right-releasing jog along the eastern margin of the Sierran microplate at the latitude of the Coso Range. Figure redrafted and modified from Unruh et al. (2008).

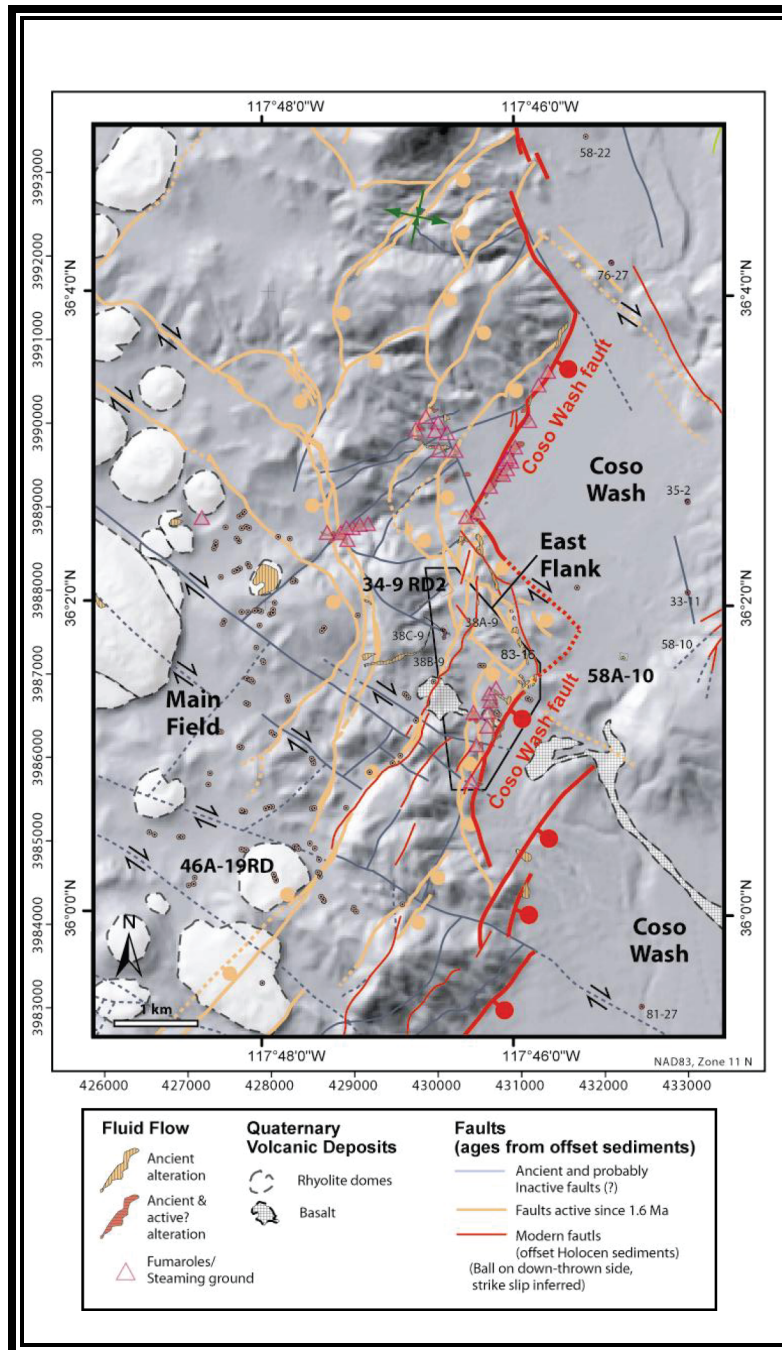


Figure 7: Tectonic map of the east flank of the Coso geothermal field over shaded relief image of topography. Figure modified from Davatzes and Hickman (2006)

## COSO GEOTHERMAL FIELD: DATA AND METHODS

Dynamic stresses from large mainshocks tend to preferentially trigger remote earthquakes in geothermal areas. Given this, the CGF presents an ideal study site to observe the interaction of dynamic stresses produced by  $M \geq 7$  earthquakes and the local stress field. Remotely triggered seismicity in the CGF has been clearly documented [e.g., *Hill et al.*, 1993; *Prejean et al.*, 2004; *Peng* 2010a; *Aiken and Peng*, 2014]. The Southern California Seismic Network (SCSN) [*Hutton et al.*, 2010] maintains an extensive catalog, to which we can compare our database of detections.

We investigate triggering at CGF and the surrounding region, implementing a combination visual inspection, detection catalog (applying the Ev1 STA/LTA algorithm), and the SCSN catalog. We identify instantaneous triggered seismicity within the wavetrain of the mainshock earthquake and or delayed triggered seismicity within 5 hours of the initial mainshock. We first generate individual databases for all 154 mainshock events from our main Antelope database. We include all available waveform data for TA and CI network stations within a 400 km radius of the CGF (Figure 8), we then apply the a 4s/40s (Ev1) STA/LTA detection algorithm [Velasco et. al, 2015] to  $\pm 5$  hours of all 154 events from 2004-2013. We compile catalog data for  $\pm 5$  hours for each of the 154 mainshock event. We also request local earthquakes in a box defined as  $35.5^{\circ}\text{N}$ – $36.5^{\circ}\text{N}$ ,  $119^{\circ}\text{W}$ – $117^{\circ}\text{W}$  with a minimum magnitude of  $M_L = 0$ . Catalog data from the Southern California Seismic Network (SCSN, network code CI) were accessed from the Southern California Earthquake Data Center (last accessed Feb. 2015, <http://scedc.caltech.edu>). We then visually inspect waveform data using detections and catalogue data as a guide to identify locally triggered events.

We compute the mainshock generated peak dynamic stress (PDS) at six seismic stations (TA-HELL, TA-R11A, CI-MPM, CI-CWC, CI-SLA, CI-CLC) following the method in Pankow et al. [2004], where peak vector velocities are computed using three-component broadband data



and multiplied by shear modulus/ Love wave group velocity ( $\mu = 33000$  MPa,  $U = 3.5$  km/s). We then average the PDS between these stations for each mainshock (Table 2). We then examine the average PDS values as a function of mainshock: magnitude, distance, depth, and back-azimuth for each triggering and non-triggering mainshock.

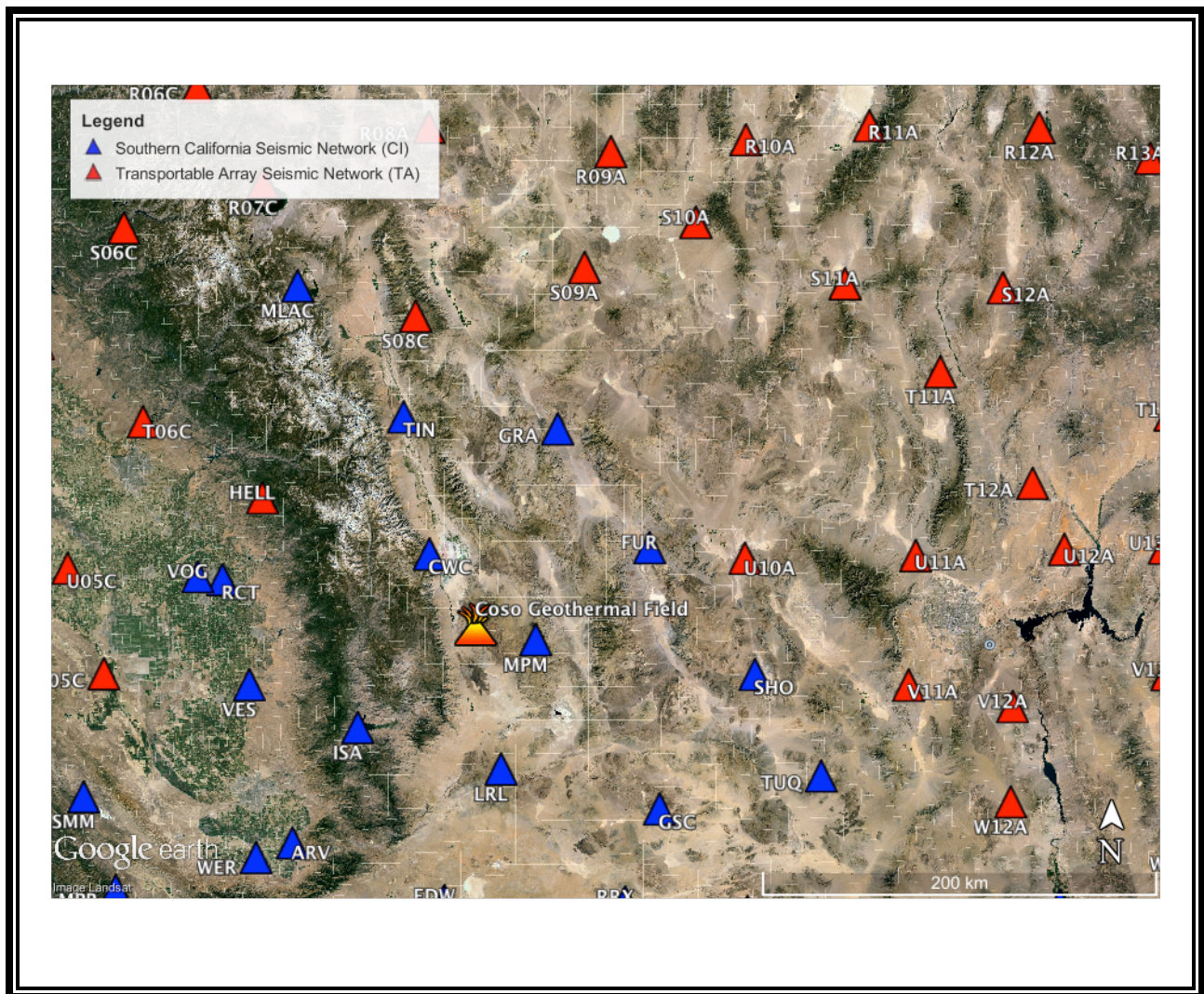


Figure 8: Google Earth satellite image of the Coso Geothermal Field and surrounding region. Red triangles indicate USArray Transportable Array (TA) station locations, blue triangles represent Southern California Seismic Network (SCSN, network code-CI) station locations. The centroid of the Coso Geothermal Field is indicated by the orange-yellow volcano shaped symbol.

Table 2: Mainshock parameters, including distance and back-azimuth, which are calculated with respect to SCSN CI-Network Code station MPM (36.06 N, -117.49 E). We compute the average mainshock generated peak dynamic stress (PDS) at six seismic stations (TA-HELL, TA-R11A, CI-MPM, CI-CWC, CI-SLA, CI-CLC). PDS values are averaged between each of the six stations. Rows Highlighted in Green indicate the mainshock triggered local seismicity in the Coso Geothermal Field or surrounding region.

Date	Time (UTC)	Lat	Lon	Mag	Depth (Km)	Distance (Km) to CI.MPM	Azimuth (Deg) CI.MPM	Back-Azimuth (Deg) to CI.MPM	Peak Dynamic Stress (PDS)
02/07/2004	02:42:34	-4.03	135.09	7.3	15	11953.2	265.805	91.2549	0.000951909
07/15/2004	04:27:13	-17.7	-178.77	7	560	6984.07	250.127	80.5988	0.000522767
07/25/2004	14:35:17	-2.49	103.97	7.3	581.9	15415.7	266.267	92.7966	0.000674331
09/05/2004	14:57:17	33.21	137.07	7.4	10	11488.3	303.906	81.2741	0.000725826
09/05/2004	10:07:07	33.07	136.73	7	18.7	11454.5	304.004	81.437	0.000598295
11/11/2004	21:26:42	-8.15	124.74	7.4	23.1	13076.8	260.867	94.2415	0.001028384
11/15/2004	09:06:55	4.74	-77.47	7.2	15	4480.49	82.7011	264.417	0.001352797
11/22/2004	20:26:23	-46.5	164.83	7	7.6	9075.34	223.026	81.0269	0.000775071
11/26/2004	02:25:00	-3.65	135.41	7	5.1	11918.6	266.207	91.1146	0.000730408
11/28/2004	18:32:12	42.9	145.21	7	42.8	10615.3	312.941	85.0335	0.001738581
12/23/2004	14:59:00	-49.71	161.58	8	10	9365	220.124	83.0775	0.006890485
12/26/2004	00:58:52	3.41	95.9	9.1	26.1	16303.9	276.139	84.8775	0.028128087
02/05/2005	12:23:18	5.29	123.44	7	540.4	13240.1	276.007	87.0853	0.000225805
03/02/2005	10:42:09	-6.57	129.88	7.1	197.6	12520.9	262.934	92.7129	0.000420858
03/28/2005	16:09:35	2.1	97.11	8.1	30	16179.9	273.67	86.9796	0.007146753
06/13/2005	22:44:32	-19.92	-69.22	7.8	111.9	5702.12	115.75	286.809	0.005804851
06/15/2005	02:50:55	41.45	-125.58	7.1	18	4664.88	350.885	167.835	0.069235226
07/24/2005	15:42:05	7.91	92.15	7.1	17.5	16634.4	285.593	76.4892	0.001298649
08/16/2005	02:46:26	38.2	142.11	7	37.8	10929.1	308.475	83.5507	0.000770446



09/09/2005	07:26:42	-4.56	153.48	7.4	93.8	9911.27	265.47	89.9235	0.11648992
09/26/2005	01:55:37	-5.74	-76.48	7.5	129.1	4601.29	98.6519	276.518	0.002978745
10/08/2005	03:50:35	34.52	73.64	7.3	7.9	16042.6	344.224	19.2248	0.002866493
01/02/2006	06:10:48	-61.01	-21.65	7.1	10	10335	150.973	264.897	0.001089995
01/02/2006	22:13:40	-19.97	-178.11	7.1	584.1	6959.68	247.5	79.1791	0.000437189
01/27/2006	16:58:54	-5.45	128.19	7.5	403.6	12713.4	264.063	92.4417	0.001039623
02/22/2006	22:19:09	-21.31	33.55	7	16.4	16104.8	128.667	236.862	0.00155586
04/20/2006	23:25:02	61.04	167.1	7.3	26.6	9234.93	331.668	102.81	0.004552836
05/03/2006	15:26:39	-20.16	-174.14	7.9	53.5	6557.25	246.416	77.294	0.006180815
05/16/2006	10:39:23	-31.84	-179.15	7.4	156	7366.15	234.976	74.191	0.002812005
07/17/2006	08:19:26	-9.32	107.42	7.2	20	14955.5	256.998	99.1687	0.000779884
08/20/2006	03:41:45	-61.02	-34.29	7	0.5	9650.76	151.028	275.947	0.00085041
11/15/2006	11:14:14	46.68	153.21	8.3	12.2	9965.23	316.49	90.5069	0.007581712
12/26/2006	12:26:21	21.86	120.54	7	6.6	13298.7	295.162	76.9896	0.00048633
01/13/2007	04:23:23	46.23	154.5	8.1	22.5	9865.11	316.055	91.432	0.019001692
01/21/2007	11:27:44	1.08	126.36	7.5	23.5	12929.4	271.195	89.4733	0.00157559
03/25/2007	00:40:03	-20.57	169.35	7.1	36.2	8265.53	248.721	83.9654	0.00092128
04/01/2007	20:39:56	-8.45	157.03	8.1	9.5	9521.15	261.58	89.339	0.007198832
08/01/2007	17:08:55	-15.67	167.7	7.2	149.5	8391.42	253.895	85.8321	0.000998905
08/08/2007	17:05:06	-5.89	107.45	7.4	295.8	15001.8	261.746	95.8329	0.001542557
08/15/2007	23:40:58	-13.38	-76.56	8	41.2	4749.95	109.832	284.852	0.0128186
09/02/2007	01:05:19	-11.59	165.82	7.2	37.5	8567.59	258.177	87.2965	0.003150703
09/12/2007	11:10:26	-4.46	101.4	8.5	35.5	15774.7	265.798	93.3001	0.006445037
09/12/2007	23:49:04	-2.62	100.73	7.9	36	15684.9	262.965	95.4705	0.005177511
09/13/2007	03:35:28	-2.16	99.57	7.1	20	15906.3	266.443	92.8382	0.00614856
09/28/2007	13:38:57	22.01	142.71	7.5	253.5	11030.6	292.169	86.3171	0.00604742
09/30/2007	05:23:34	-49.25	164.19	7.4	10	10753.4	280.542	88.7749	0.0018636
09/30/2007	02:08:31	10.54	145.8	7	18.5	9170.26	220.348	81.1252	0.0018636
10/31/2007	03:30:18	18.96	145.38	7.2	221.9	10769.9	288.978	87.6863	0.00580915
11/14/2007	15:40:49	-22.32	-69.78	7.7	33.6	5728.36	118.866	288.957	0.003780075
11/29/2007	19:00:19	14.99	-61.22	7.4	147.3	6405.9	72.2653	260.262	0.001223833
12/09/2007	07:28:20	-26.1	-177.36	7.8	149.8	7032.07	240.637	75.7515	0.004642827
12/19/2007	09:30:28	51.4	-179.54	7.2	36.2	8118.15	324.628	112.468	0.001939075
02/20/2008	08:08:31	2.76	95.96	7.3	31.4	16303	274.965	85.8588	0.001144171
02/25/2008	08:36:33	-2.49	99.92	7.2	29.8	15865.5	265.933	93.2295	0.00096269
03/20/2008	22:32:58	35.55	81.51	7.1	10	15634.5	335.362	30.7457	0.001119035
04/09/2008	12:46:12	-20.04	168.91	7.3	31.4	8305.25	249.309	84.2751	0.001356333
04/12/2008	00:30:12	-55.59	158.54	7.1	10	9638.27	214.441	85.0308	0.001012874
05/12/2008	06:27:59	31.06	103.37	7.9	7.6	14523.8	312.442	59.3093	0.009771979
07/05/2008	02:12:06	53.95	152.86	7.7	646.1	9995.84	323.767	90.2815	0.003856144
11/16/2008	17:02:32	1.35	122.16	7.3	28.1	13396.5	271.554	89.2149	0.00067138

11/24/2008	09:03:00	54.22	154.29	7.3	505.3	9902.51	324.05	91.4401	0.00086155
01/03/2009	22:33:42	-0.71	133.31	7.2	34.4	12235.2	269.44	90.1907	0.001580922
01/03/2009	19:43:55	-0.53	132.6	7.4	31.1	12156.1	269.253	90.2456	0.00236238
01/15/2009	17:49:38	46.83	155.25	7.3	31.1	9809.49	316.671	91.992	0.002960232
02/11/2009	17:34:51	3.78	126.5	7.1	24.2	12907.7	274.177	88.1697	0.000878606
03/19/2009	18:17:40	-23.16	-174.59	7.6	30.9	6679.92	243.157	75.8029	0.001979349
05/28/2009	08:24:48	16.81	-86.24	7.3	29	3899.6	59.9519	244.654	0.016658235
07/15/2009	09:22:31	-45.83	166.64	7.8	20.9	8924.84	223.483	79.7981	0.001907862
08/09/2009	10:55:56	33.15	138.06	7.1	302.2	11364	303.821	82.0159	0.000925952
08/10/2009	19:55:39	14.05	92.87	7.5	30.7	16349.1	296.189	67.6154	0.001251789
09/02/2009	07:55:01	-7.73	107.41	7	57.8	14982.3	259.186	97.6374	0.000889204
09/29/2009	17:48:11	-15.51	-171.94	8.1	18.5	6223.9	251.284	79.2478	0.026917685
09/30/2009	10:16:10	-0.71	99.97	7.6	90.2	15867	268.841	90.9204	0.001625302
10/07/2009	23:13:49	-13.08	166.46	7.4	32.9	8501.96	256.662	86.8032	0.006547865
10/07/2009	22:18:53	-12.47	166.37	7.8	59	8512.63	257.251	86.97	0.006547865
10/07/2009	22:03:14	-13.04	166.5	7.6	33.7	8506.54	256.624	86.8031	0.006547865
11/09/2009	10:44:54	-17.27	178.45	7.3	591.3	7268.69	251.047	81.8326	0.000519495
01/03/2010	22:36:29	-8.88	157.42	7.1	29.8	9478.81	261.147	89.2454	0.000981646
01/12/2010	21:53:10	18.38	-72.59	7	15	5312.98	64.9403	252.54	0.013277649
02/26/2010	20:31:26	25.98	128.51	7	24.2	12409.6	297.917	79.0217	0.001555469
02/27/2010	06:34:13	-36.15	-72.93	8.8	28.1	6027.12	138.915	303.895	0.02660814
02/27/2010	08:01:23	-37.84	-75.21	7.4	35	6098.33	135.964	300.813	0.026608272
03/11/2010	14:55:29	-34.29	-71.8	7	24.4	6085.21	133.428	298.699	0.0008014
04/04/2010	22:40:43	32.28	-115.26	7.2	5.2	3581.78	3.547	184.188	0.275735931
04/06/2010	22:15:02	2.36	97.11	7.8	33.4	16178.3	274.124	86.6067	0.001852559
05/09/2010	05:59:42	3.73	96.03	7.3	42.3	16286.2	276.688	84.4278	0.000496037
05/27/2010	17:14:46	-13.67	166.67	7.2	34.7	8487.58	256.009	86.6096	0.000796068
06/12/2010	19:26:50	7.85	91.95	7.5	31.4	16657.4	285.57	76.4818	0.00190963
06/16/2010	03:16:29	-2.2	136.59	7	22.1	11789.8	267.728	90.6232	0.000768485
07/18/2010	13:35:00	-6.04	150.66	7.3	43.1	10223.7	263.997	90.1935	0.001965414
07/23/2010	23:15:09	6.74	123.33	7.5	633.7	13225.5	277.612	86.3155	0.002063532
07/23/2010	22:51:13	6.42	123.58	7.7	584.7	13217.6	277.278	86.4867	0.002064046
07/23/2010	22:08:11	6.71	123.49	7.3	610.2	13243	277.658	86.2748	0.002063702
08/10/2010	05:23:46	-17.53	168.04	7.3	33.5	8371.25	251.962	85.2448	0.001476788
08/12/2010	11:54:15	-1.28	-77.37	7.1	206.5	4467.91	91.9727	271.508	0.000868994
09/03/2010	16:35:46	-43.36	171.9	7	4	8458.95	225.161	76.4622	0.000291494
09/29/2010	17:11:24	-4.99	133.78	7	20.5	12095.8	264.768	91.6782	0.000120228
10/25/2010	14:42:22	-3.52	100.1	7.8	20	15837.8	264.28	94.5298	0.000620282
12/21/2010	17:19:40	26.9	143.7	7.4	14	10894	297.019	86.0098	0.002584838
12/25/2010	13:16:37	-19.7	167.95	7.3	16	8401.75	249.747	84.7126	0.002476037
01/01/2011	09:56:58	-26.8	-63.14	7	576.8	6523.82	121.695	287.832	0.000439329

01/02/2011	20:20:17	-38.36	-73.33	7.1	24	6196.93	138.454	302.475	0.000517332
01/18/2011	20:23:23	28.78	63.95	7.2	68	16848.2	357.365	3.00227	0.000773355
03/09/2011	02:45:20	38.44	142.84	7.3	32	10862.7	308.652	83.9771	0.073477319
03/11/2011	06:25:50	38.06	144.59	7.6	18.6	10905.2	308.552	83.7002	0.031109647
03/11/2011	06:15:40	36.28	141.11	7.9	42.6	11041.9	306.642	83.2248	0.031109699
03/11/2011	05:46:24	38.3	142.37	9	29	10714	308.14	85.1178	0.031109689
04/07/2011	14:32:43	38.28	141.59	7.1	42	10973.4	308.603	83.2115	0.00086303
06/24/2011	03:09:39	52.05	-171.84	7.3	52	7670.51	327.462	119.428	0.004170384
07/06/2011	19:03:18	-29.54	-176.34	7.6	17	7036.27	236.666	73.4861	0.009762159
07/10/2011	00:57:10	38.03	143.26	7	23	10830.7	308.207	84.2936	0.001320038
08/20/2011	18:19:23	-18.31	168.22	7.1	28	8368.61	251.093	84.9919	0.001540841
08/20/2011	16:55:02	-18.37	168.14	7.2	32	8359.6	251.148	84.9808	0.001540841
08/24/2011	17:46:11	-7.64	-74.53	7	147	4841.9	101.063	278.073	0.000798595
09/03/2011	22:55:40	-20.67	169.72	7	185.1	8228.35	248.58	83.7971	0.00054425
09/15/2011	19:31:04	-21.61	-179.53	7.3	644.6	7139.3	245.988	79.0016	0.000458186
10/21/2011	17:57:16	-28.99	-176.24	7.4	33	7009.71	237.228	73.6918	0.00507078
10/23/2011	10:41:22	38.72	43.51	7.3	16	15328.8	22.2368	331.068	0.001696676
12/14/2011	05:04:59	-7.56	146.8	7.1	140.9	10649.1	262.453	90.7489	0.0007128
01/10/2012	18:36:59	2.43	93.21	7.2	19	16610.7	274.72	85.9426	0.00061983
03/14/2012	09:08:35	40.89	144.94	7	12	10657	310.948	85.0464	0.000925183
03/20/2012	18:02:47	16.49	-98.23	7.4	20	2792.23	48.2839	231.083	0.055302541
03/25/2012	22:37:06	-35.2	-72.22	7.1	40.7	6100.83	134.605	299.618	0.001358723
04/11/2012	10:43:10	0.8	92.46	8.2	25.1	16702.6	271.591	88.6211	0.025105815
04/11/2012	08:38:36	2.33	93.06	8.6	20	16628.1	274.546	86.0857	0.025186717
04/12/2012	07:15:48	28.7	-113.1	7	13	3211.1	8.01021	189.127	0.029198688
08/14/2012	02:59:38	49.8	145.06	7.7	583.2	10555.4	319.85	84.3115	0.003854235
08/27/2012	04:37:19	12.14	-88.59	7.4	28	3463.53	66.1479	249.266	0.015814505
08/31/2012	12:47:33	10.81	126.64	7.6	28	12844.7	281.903	84.8364	0.005002687
09/05/2012	14:42:07	10.09	-85.32	7.6	35	3732.98	71.6345	254.532	0.015341917
09/30/2012	16:31:35	1.93	-76.36	7.2	170	4582.57	87.0868	267.806	0.001337575
10/28/2012	03:04:08	52.79	-132.1	7.8	14	6012.16	349.085	161.834	0.021059563
11/07/2012	16:35:46	13.99	-91.9	7.3	24	3216.62	60.1884	243.36	0.018488655
12/07/2012	08:18:23	37.89	143.95	7.3	31	10771.8	308.015	84.7398	0.003197728
12/10/2012	16:53:08	-6.53	129.83	7.1	155	12526.6	262.975	92.7031	0.000361869
01/05/2013	08:58:19	55.39	-134.65	7.5	10	6341.2	348.415	159.393	0.021417886
02/06/2013	01:54:14	-10.5	165.59	7	8.8	8641.19	259.012	87.6173	0.005368167
02/06/2013	01:23:19	-11.18	164.88	7.1	10	8668.07	258.636	87.5809	0.005368167
02/06/2013	01:12:25	-10.8	165.11	7.9	24	8587.32	259.297	87.5914	0.005368157
02/08/2013	15:26:38	-10.93	166.02	7.1	21	8542.4	258.84	87.4086	0.001304938
04/06/2013	04:42:35	-3.52	138.48	7	66	11577.8	266.396	90.8732	0.000526982
04/16/2013	10:44:20	28.03	62	7.7	80	16934.6	0.96620	358.907	0.004550144

04/19/2013	03:05:52	46.22	150.79	7.2	110	10151.8	316.041	88.7613	0.001402128
05/23/2013	17:19:04	-23.01	-177.23	7.4	173.7	6939.21	243.97	77.2243	0.00204213
05/24/2013	05:44:48	54.89	153.22	8.4	598.1	9973.2	324.711	90.5787	0.015103699
07/07/2013	18:35:30	-3.92	153.92	7.3	386.3	9862.31	266.105	89.9043	0.001018847
07/15/2013	14:03:39	-60.83	-25.17	7.3	11	10145.2	150.686	267.978	0.0005596
08/30/2013	16:25:02	51.61	-175.36	7	33.5	7862.76	325.961	116.149	0.00192539
09/24/2013	11:29:48	27	65.51	7.7	20	17032	354.098	6.61772	0.004836334
09/25/2013	16:42:43	-15.85	-74.56	7	45.8	5030.97	112.493	286.267	0.001221542
10/15/2013	00:12:37	9.77	124.02	7.2	56.8	13141	281.012	84.7718	0.00192539
10/25/2013	17:10:16	37.19	144.66	7.3	10	10715.9	307.265	85.2557	0.004836334
11/17/2013	09:04:55	-60.3	-46.36	7.8	10	8987.02	151.482	286.511	0.002431775
11/25/2013	06:27:33	-53.88	-54.88	7	10	8259.26	146.884	292.664	0.001221542

## **COSO GEOTHERMAL FIELD: TRIGGERING MAINSHOCKS**

We examined local triggering in the Coso Geothermal Field, from 154 remote mainshocks ( $M \geq 7$ ). For each mainshock, we compare post-mainshock seismicity with pre-mainshock background levels. Of the original 154 mainshocks in our study, we eliminate 120 of the mainshocks where the local post-mainshock seismicity rate is constant or decreases relative to the pre-mainshock rates. The remaining 34 mainshocks have moment magnitudes ranging from 7.0 to 8.8 and depths of 10 to 598.1 km. We hypothesize that these 34 mainshocks (22% of those examined) triggered local seismicity in the 5 hours following the mainshock. The our auto-detection and the SCSN catalog indicate that 16 mainshocks instantaneously (within the wavetrain of the mainshock) triggered local seismicity; 18 mainshocks triggered seismicity that was delayed by within  $\sim 1$ -5 hours of the mainshock (Table 3). An investigation of the potential seismic triggering phases is compiled in Table 3. A majority of instantaneously triggered earthquakes identified are in phase with the passing of surface waves, without a time delay. Of note, we find a magnitude 6.9 mainshock earthquake on July, 18 2010 at 13:04:11 UTC, in the New Britain Region, Papua New Guinea instantaneously triggered seismicity in the CGF in phase with the arrival of the mainshocks *S*-wave and Rayleigh waves. We included this event although it was below our  $M \geq 7$  magnitude cut off, and note that it occurred  $\sim 30$  minutes prior to a magnitude 7.3 mainshock. Both mainshocks originated from the same region (New Britain Region, Papua New Guinea) and appear to have instantaneosly triggered seismicity in the CGF. We include the  $M = 6.9$  mainshock in Table 3, however it is excluded from further analysis.

Of the 16 cases of assumed instantaneous triggering 8 (50%) of the triggered events displayed no activity in the CGF or its vicinity within 5 hours prior to the mainshock rupture. Of the 18 delayed triggered events 3 (17%) of the triggered events displayed no prior activity within 5 hours prior to passage of the mainshock coda. The cases of assumed triggered seismicity that

display pre-mainshock activity account for 68% of our total triggered catalog, and we find activity in the 5-hours post-mainshock display a rapid increase in the frequency and magnitude of seismicity in the study area. This suggests the propagating dynamic stresses of the seismic waves generated from the mainshock excited the system, therefore increasing seismic activity. We identify 147 local events ranging in magnitude ( $M_L$ ) 0.02-3.45 (Figure 9) triggered within 5 hours following 34 ( $M_W \geq 7.0$ ). Of the 147 local events we find 17 events that had not been previously cataloged.

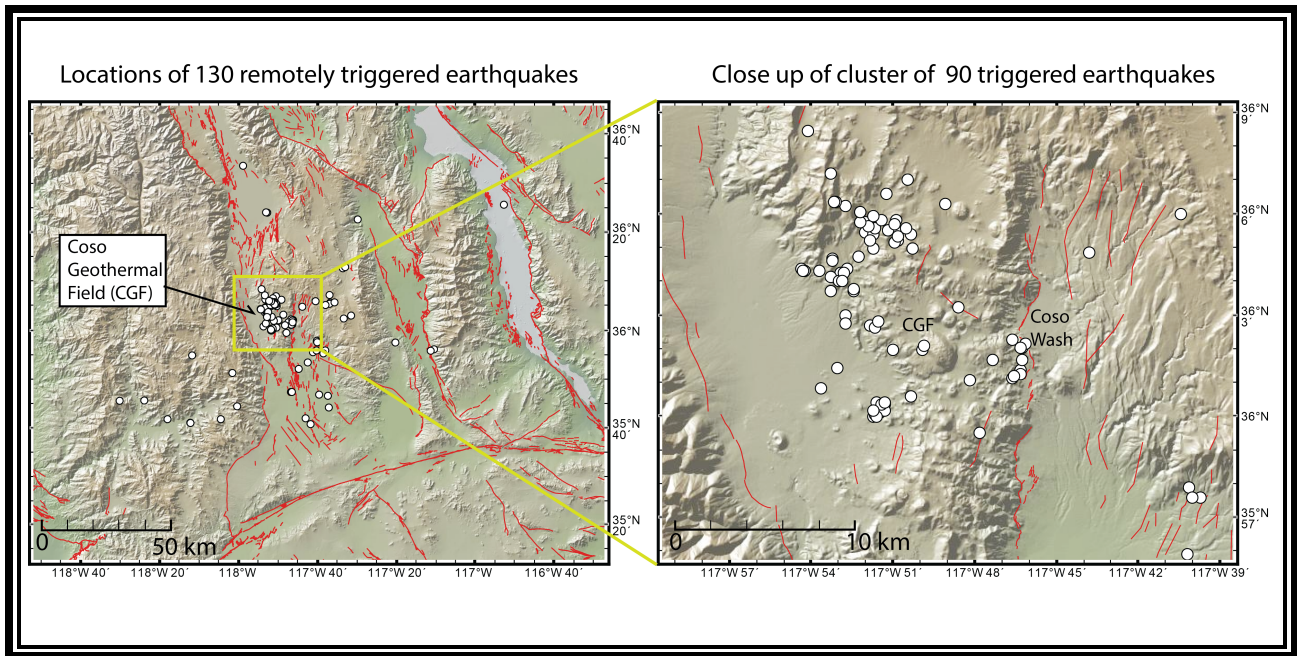


Figure 9: Map of locally triggered seismicity in the Coso geothermal field and surrounding study area. On the left white circles indicate locations of 130 remotely triggered local seismicity, cataloged and located by the Southern California Earthquake Center, events range in magnitude ( $M_L$ ) 0.02-3.45, red lines indicate quaternary faults. On the right we zoom into a cluster of seismicity in the Coso Geothermal Field. The white circles indicate locations of 90 remotely triggered local seismicity, cataloged and located by the Southern California Earthquake Center, events range in magnitude ( $M_L$ ) 0.02-3.45, red lines indicate quaternary faults.

Table 3: Mainshock parameters of our set of 34  $M \geq 7$  “Triggering Mainshocks”, including one additional triggering mainshock of  $M=6.9$ . We compute distance and back-azimuth, with respect to SCSN CI-Network Code station MPM (36.06 N, -117.49 E) located 30 km from the center of the Coso Geothermal Field (36.03N, -117.82E). We calculate the average mainshock generated peak dynamic stress (PDS) at six seismic stations (TA-HELL, TA-R11A, CI-MPM, CI-CWC, CI-SLA, CI-CLC). PDS values are an average of the PDS from all six stations. The table also includes information about if the locally triggered seismicity is assumed to be consistent with triggering that is instantaneous or delay. We indicate which phases of the mainshocks wavetrain is the assumed triggering factor (P=P-Wave, S=S-Wave, L=Love Wave, R=Rayleigh Wave, C=coda of the mainshock). We also indicate whether the Coso Geothermal field or anywhere in our Coso study area (35.5°N–36.5°N, 119°W–117°W) exhibited seismicity in the 5-hours prior to the passage of the mainshock earthquake (Y=Yes, there was seismicity cataloged prior to the mainshock earthquake; N=No, there was not seismicity cataloged prior to the mainshock earthquake).

Date	Time (UTC)	Mag	Depth (km)	Distance (Km) to CI.MPM	Back-azimuth (Deg) to CI.MPM	Avg PDS (Mpa)	Instant or Delay?	Trig Phase	Prior Seismicity ?
07/24/2005	15:42:05	7.1	17.5	16634.4	76.4892	0.001298649	Instant	S	Y
09/26/2005	1:55:37	7.5	129.1	4601.29	276.518	0.002978745	Delay	--	Y
01/02/2006	6:10:48	7.1	10	10335	264.897	0.001089995	Instant	L	N
05/03/2006	15:26:39	7.9	53.5	6557.25	77.294	0.006180815	Delay	--	Y
07/17/2006	8:19:26	7.2	20	14955.5	99.1687	0.000779884	Instant	C,R	N
09/12/2007	11:10:26	8.5	35.5	15774.7	93.3001	0.006445037	Instant	C,R	N
09/13/2007	3:35:28	7.1	20	15906.3	92.8382	0.00614856	Delay	--	N
04/12/2008	0:30:12	7.1	10	9638.27	85.0308	0.001012874	Instant	C,R	N
02/11/2009	17:34:51	7.1	24.2	12907.7	88.1697	0.000878606	Instant	R	Y
08/09/2009	10:55:56	7.1	302.2	11364	82.0159	0.000925952	Instant	S	N
09/29/2009	17:48:11	8.1	18.5	6223.9	79.2478	0.026917685	Delay	--	N



01/03/2010	22:36:29	7.1	29.8	9478.81	89.2454	0.000981646	Instant	R	Y
01/12/2010	21:53:10	7	15	5312.98	252.54	0.013277649	Delay	--	Y
02/27/2010	6:34:13	8.8	28.1	6027.12	303.895	0.02660814	Instant	S,L	Y
04/06/2010	22:15:02	7.8	33.4	16178.3	86.6067	0.001852559	Instant	R	N
05/09/2010	5:59:42	7.3	42.3	16286.2	84.4278	0.000496037	Delay	--	Y
07/18/2010	13:04:11	6.9	42	--	--	--	Instant	S,R	
07/18/2010	13:35:00	7.3	43.1	10223.7	90.1935	0.001965414	Instant	L	Y
12/21/2010	17:19:40	7.4	14	10894	86.0098	0.002584838	Delay	--	Y
06/24/2011	3:09:39	7.3	52	7670.51	119.428	0.004170384	Delay	--	Y
07/06/2011	19:03:18	7.6	17	7036.27	73.4861	0.009762159	Delay	--	Y
08/20/2011	18:19:23	7.1	28	8368.61	84.9919	0.001540841	Delay	--	Y
08/24/2011	17:46:11	7	147	4841.9	278.073	0.000798595	Instant	R	N
10/21/2011	17:57:16	7.4	33	7009.71	73.6918	0.00507078	Delay	--	Y
03/20/2012	18:02:47	7.4	20	2792.23	231.083	0.055302541	Delay	--	Y
08/31/2012	12:47:33	7.6	28	12844.7	84.8364	0.005002687	Delay	--	N
11/07/2012	16:35:46	7.3	24	3216.62	243.36	0.018488655	Delay	--	Y
12/07/2012	8:18:23	7.3	31	10771.8	84.7398	0.003197728	Instant	S,R	N
12/10/2012	16:53:08	7.1	155	12526.6	92.7031	0.000361869	Instant	R	Y
04/06/2013	4:42:35	7	66	11577.8	90.8732	0.000526982	Instant	S,R	Y
04/16/2013	10:44:20	7.7	80	16934.6	358.907	0.004550144	Delay	--	Y
05/23/2013	17:19:04	7.4	173.7	6939.21	77.2243	0.00204213	Delay	--	Y
05/24/2013	5:44:48	8.4	598.1	9973.2	90.5787	0.015103699	Delay	--	Y
07/15/2013	14:03:39	7.3	11	10145.2	267.978	0.0005596	Instant	R	Y
11/17/2013	9:04:55	7.8	10	8987.02	286.511	0.002431775	Delay	--	Y



## **COSO GEOTHERMAL FIELD: MAINSHOCK PARAMETERS**

The locations and mechanisms of the 154 mainshock events we study vary throughout the highly seismogenic regions of the world (Figure 10). Several are concentrated near the western edge of the Pacific Plate, a naturally more seismically active area. Notably, the majority of triggering mainshocks exhibit a thrust mechanism (Figure 10), although based on the similarities between the locations and mechanisms of triggering and non-triggering mainshocks, we do not assign any region as a preferential trigger locality specific to the CGF region.

We find the average mainshock PDS values, for both non-triggering mainshocks and triggering mainshocks (Figure 11) range between values of ( $10^{-3}$ – $10^{-1}$  MPa). As expected, there is a general trend of larger PDS values corresponding to larger magnitudes, although we find several Mw 7-7.5 mainshocks that deviate from this trend, producing PDS values as high as 0.17 MPa, a value more consistent with a magnitude 9 mainshock. The highest value PDS values we computed was  $\sim 0.3$  MPa for non-triggering events and  $\sim 0.06$  MPa for triggering events. The lowest PDS we computed for a triggering event is  $\sim 0.0005$  MPa a small value implying relatively weak triggering, which is consistent with the finding of Aiken and Peng (2014) who indicate geothermal sites in California are susceptible to a triggering threshold of  $<0.001$  MPa.

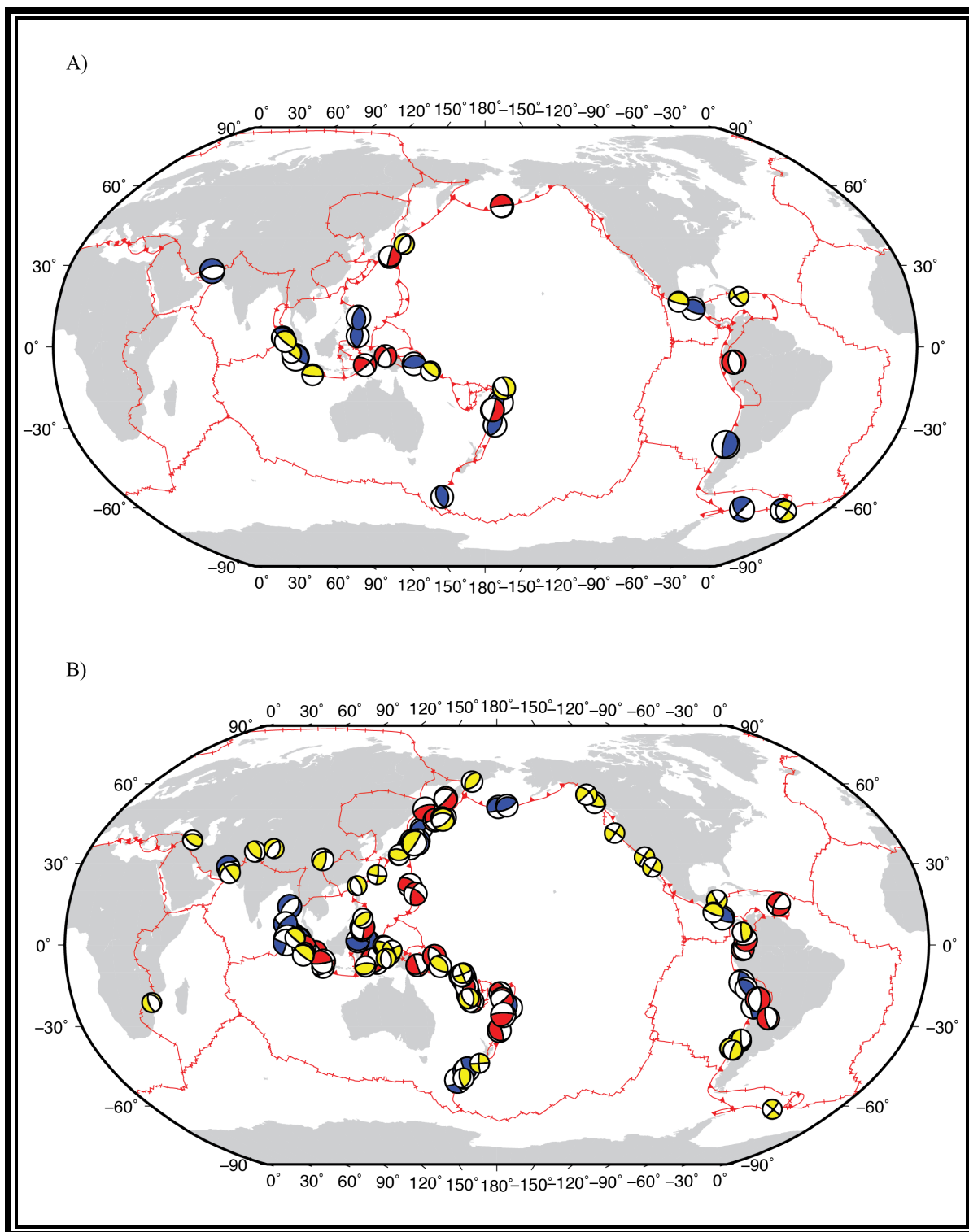


Figure 10: World map of 154 mainshocks in our study and beach-balls to indicate their mechanisms, color coded by depth. Shallow source (0-20km) depth mainshocks are indicated by yellow mechanisms; mainshocks with a source depth between (21-70km) are indicated by blue mechanisms, mainshocks with a source depth of (71km-600km) are indicated by red mechanisms. A) World map indicating locations and mechanisms of 34 triggering mainshocks, these events triggered remote seismicity in the Coso Geothermal Field and surrounds region. B) World map indicating locations and mechanisms of 120 non-triggering mainshocks.

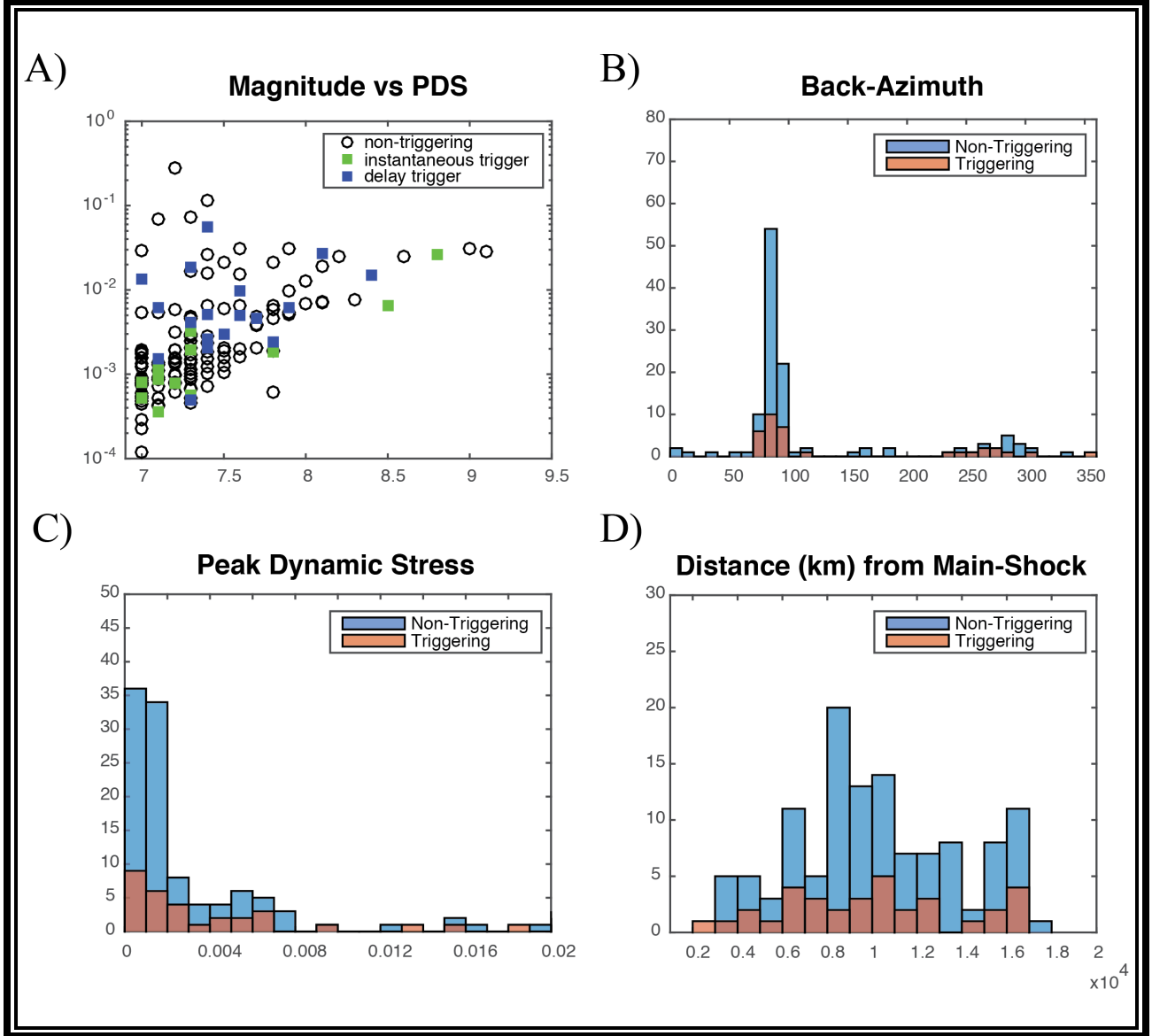


Figure 11: A) Scatter plot of Peak Dynamic Stress (PDS) (Y-axis) against Mainshock Magnitude) (X-Axis), black circles indicate 120 non-triggering mainshocks, green squares represent 16 mainshocks that instantaneously triggered local seismicity in the Coso geothermal field, blue squares represent 18 mainshocks that induced a delayed triggering of local seismicity in the Coso Geothermal field. B) Histogram of stacked mainshock back-azimuths plotted in 10 degree bins, orange indicated triggering mainshocks, blue indicates non-triggering mainshocks. C) Histogram of stacked mainshock generated PDS plotted in 0.001 MPa bins, orange indicated triggering mainshocks, blue indicates non-triggering mainshocks. D) Histogram of stacked distances from Mainshock to CI-network station MPM plotted in 1000 km bins, orange indicated triggering mainshocks, blue indicates non-triggering mainshocks.

## Discussion

In this study of 154 mainshock events, we observe mainshocks upwards of 10,000 km away capable of triggering remote seismicity in the CGF. This is consistent with prior documentation of triggering in the far-field [e.g., *Hill and Prejean*, 2014 and references therein]. We find 147 locally triggered earthquakes following 34 of the 154 mainshocks studied, indicating that dynamic earthquake triggering in the region of the CGF is quite common. Of our 147 local triggered earthquakes 33 are triggered within the wavetrain of the mainshock, 5 of these correspond to the arrival of the *S*-phase, 17 correspond to the passage of surface waves (Love and Rayleigh), 11 are triggered within the coda of the mainshock (Table 8.1). The majority of our local events occur within the first three hours after the passage of the surface waves. The time delay between the passage of dynamic stresses of the surface waves is not unexpected, several examples of delayed dynamic triggering have been previously documented [e.g., *Velasco et al.*, 2008; *Jagla*, 2011; *Morton and Bilek*, 2014].

We suggest delayed triggering in these cases may be consistent with previous hypotheses [e.g., *Hill and Prejean*, 2014 and references therein] of which the excitation of crustal fluids, in this case fluids associated with the shallow heat source of the CGF, as the cause for the delay in the triggering of local seismicity. Delayed locally triggered seismicity (Figure 12) initiated by the onset of surface wave arrivals, suggest fluid diffusion as the processes responsible for the delay in the failure of these events [e.g., *Bodin and Gomberg*, 1994; *Brodsky*, 2006; *Syracuse et al.*, 2010]. Recent documentation of dynamically triggered earthquakes indicate Rayleigh waves (which produce both longitudinal and transverse motion) can trigger events by inducing fluid excitation, or cause Coulomb failure. [*Rubinstein et al.* 2007, 2009; *Hill* 2008; *Miyazawa et al.* 2008; *Peng and Chao*, 2008; *Peng et al.*, 2008, 2009, 2010a].

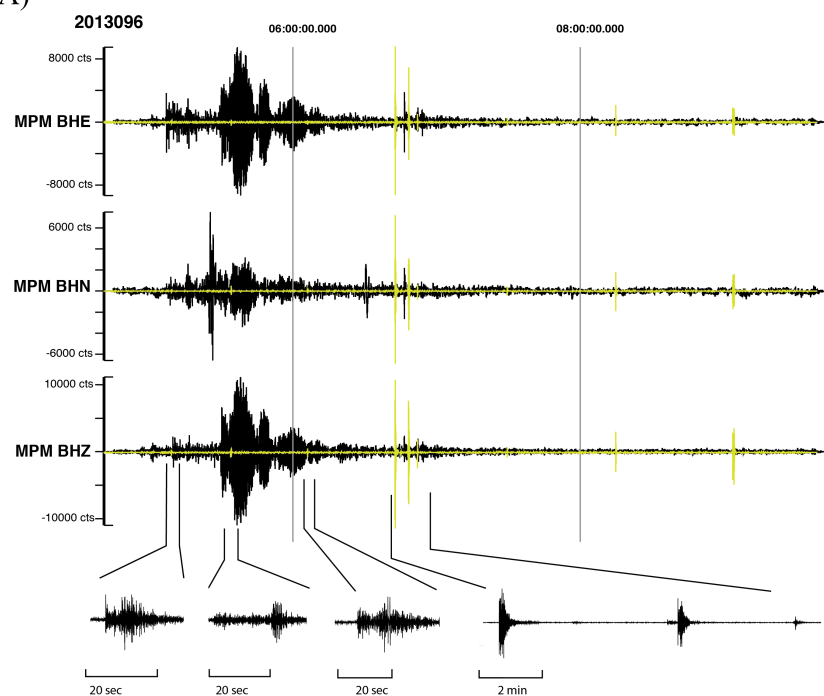
We identified 33 triggered earthquakes occurring in phase with either the early seismic arrivals or the passage of the surface waves without a time delay (Figure 12). These events may be induced by Coulomb failure [Hill, 2008; Gonzalez-Huizar and Velasco, 2010]. We identified 3 cases of Love-wave and 14 cases of Rayleigh-wave instantaneous remote triggering of local earthquake in the CGF. Both Rayleigh and Love waves can cause the failure of a fault by the Coulomb failure criteria. [Peng and Chao, 2008; Hill, 2008; Peng *et al.* 2008, 2009, 2010a]. We examine back-azimuth angles of triggering mainshocks and find several events are consistent with fault orientations in the CGF region. Consistent back-azimuth angles indicate the orientation of seismic arrival phases, either parallel or perpendicular to the local stress field (Figure 13) (Heidbach *et al.*, 2008). Back-azimuth angles are in agreement with the orientation of both active faults and borehole tensile fractures (trending N to NNE) documented by Davatzes and Hickman (2006). Our observations are consistent with those of Chao *et al.* (2013); the potential of remotely triggered seismicity is not solely dependent on the strain imposed by surface waves but their back-azimuth angles (orientations). As well previous documentation following the 1992 Landers and 2002 Denali Fault Earthquake mainshocks [Anderson *et al.*, 1994; Husker and Brodsky, 2004; Pankow *et al.*, 2004] indicate preferential triggering occurs in areas of high heat flow (i.e. geothermally active).

The general trends of mainshock parameters and PDS values show no clear indication of a triggering threshold for the CGF region, although we find the lowest PDS generated by a triggering mainshock is  $\sim 0.0005$  MPa. When comparing PDS as a function of mainshock parameters several triggering mainshocks follow similar trends as non-triggering mainshocks (Figure 11). Based on our data and findings, the initial pattern of triggering and non triggering mainshocks indicate, dynamic triggering is highly dependent on the state of the regional stress

field and dynamic stresses aligning favorably with the local stress field, not necessarily a specific threshold value of PDS generated. In future work we will determine if this initial finding is maintained after applying a series of statistical tests. If our results are confirmed, it will be consistent with the idea that a critically stressed fault can respond to the passage of dynamic stresses in a manner that invokes a clock-advance (premature failure of a fault), triggering failure of the fault [e.g., *Gomberg*, 2001; *Boese et al.*, 2014]. The stress changes imposed by passing seismic waves can alter the stress state of a fault, by slightly reducing the frictional strength, or the contact surface of a fault. If the passage of seismic waves imposes enough strain, it can initiate the immediate failure of a fault. Although in several cases point to the likelihood this strain is not enough to immediately deform the system; in which case a time delayed processed may be initiated and eventually evolves into the failure of a fault [*Parsons*, 2005; *Gonzalez-Huizar and Velasco*, 2011].

The trends produced by comparison of PDS values and mainshock parameters may be a result of irregular sampling, or a lack of mainshock events to study originating from all possible orientations (the majority of  $(M) \geq 7$  earthquakes occur in the same general regions). In addition, previous studies have found the occurrence of hundreds of dynamically triggered events following mainshock wave passage [e.g., *Hill et al.*, 1993; *Husen et al.*, 2004; *Prejean et al.*, 2004], however since we limit the time window of our study to  $\pm 5$  hours from the initial mainshock (with the exception of the Feb. 27, 2010 Offshore Bio-Bio ( $M=8.8$ ) Chile earthquake), we may not observe this high number of locally triggered events.

A)



B)

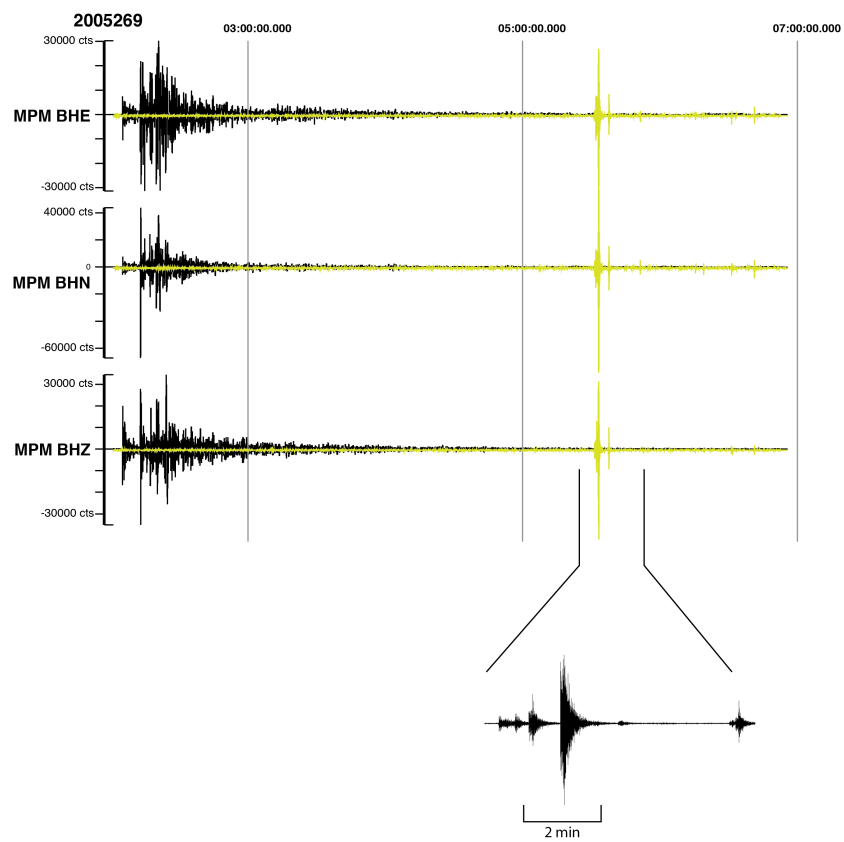




Figure 12: Instantaneous and Delayed Triggered Seismicity, originating from the Coso Geothermal Field. Raw 3-component data colored black, yellow waveforms on top represent a 5Hz highpass of the raw data. We zoom into and display locally triggered earthquakes originating from the Coso Geothermal Field (CGF). A) 3-component waveform data from CI-network station MPM, capturing the 04/06/2013 04:42:35-UTC Mw=7.0 Irian Jaya, Indonesia earthquake and instantaneously triggered seismicity originating from the CGF study area. B) 3-component waveform data from CI-network station MPM, capturing the 09/26/2005 01:55:37-UTC Mw=7.5 Northern Peru earthquake and delayed triggered seismicity originating from the CGF study area.

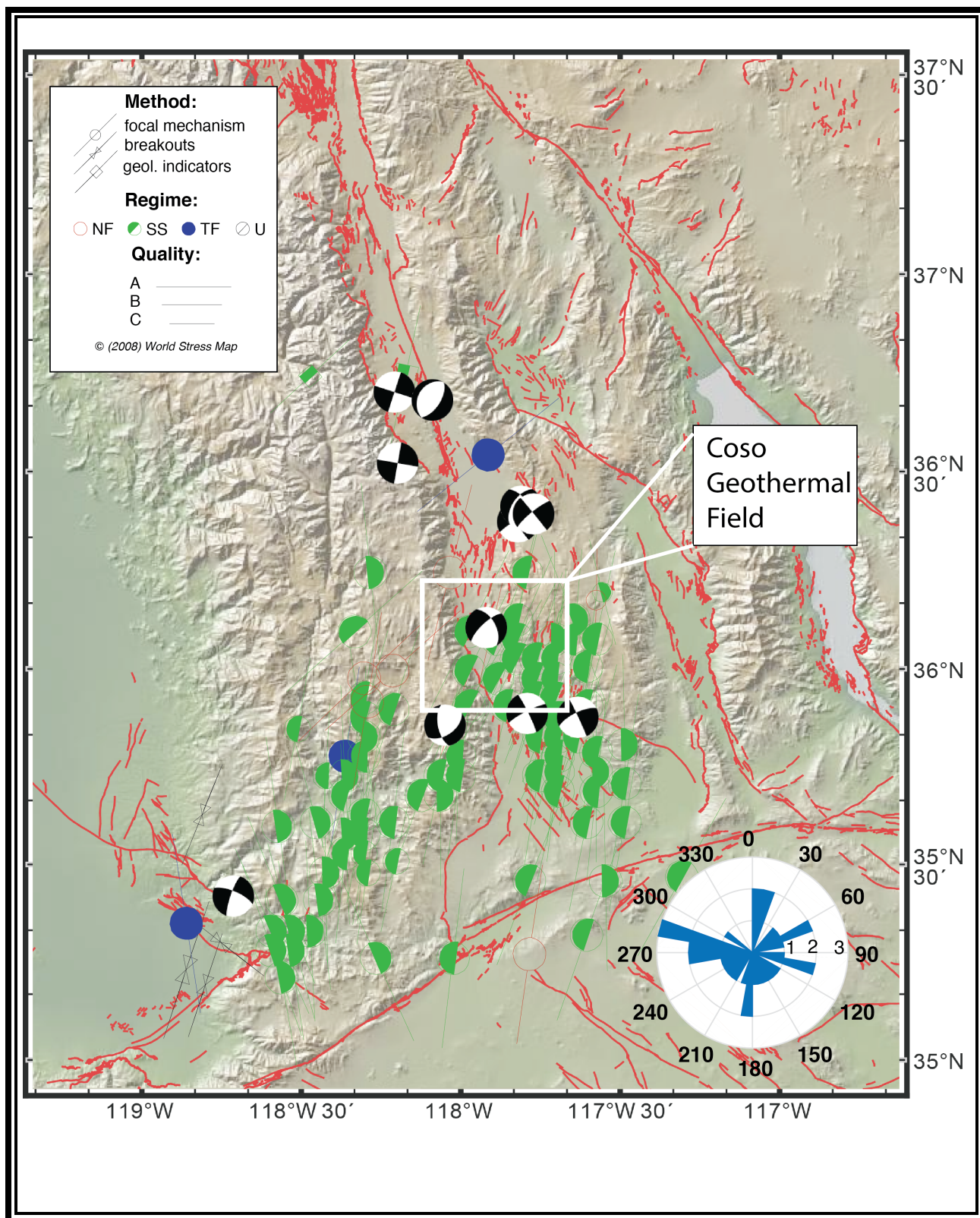


Figure 13: Map of southern California, we display focal mechanisms and stress data within our study area ( $35.5^{\circ}\text{N}$ – $36.5^{\circ}\text{N}$ ,  $119^{\circ}\text{W}$ – $117^{\circ}\text{W}$ ). The blue rose plot indicates the back-azimuth angles of 34 triggering mainshocks; back-azimuth angles are stacked and plotted in bins of 10 degrees. Stress data retrieved from The World Stress Map database (via , last accessed 04/2015). Stress map data indicates the local in the stress field for our study area. The white box indicates the Coso Geothermal Field. Focal mechanisms (white and black beach balls) were retrieve from the Global Centroid Moment Tensor Project (<http://www.globalcmt.org>, last accessed 04/2015). We find remote triggering is enhanced by the orientation (back-azimuth) of the passing seismic waves. We find several events align favorably (parallel and perpendicular) with the local stress field and/or orientation of faults in the CGF triggered region.

## Conclusion

Of 154 mainshocks ( $M \geq 7$ ) studied 34 mainshocks (22%) triggered local seismicity in the CGF region by imposing a transfer of dynamic stress. The CGF responded to the 34 mainshocks, displaying an increase in the magnitude and frequency (rate) from pre-mainshock to post-mainshock seismicity. We observe both instantaneous (16 events) and delayed (18 events) triggering of local seismicity from the  $\pm 5$  hours of the mainshock. We find remote triggering is enhanced by the orientation (back-azimuth) of the passing seismic waves. We find several events align favorably with the local stress field and/or orientation of faults in the CGF triggered region.

The CGF contains active fault systems and fluid processes which accounts for the high rate of background seismicity and this contributes to the CGF's susceptibility to dynamic triggering [Hill and Prejean, 2014]. Our findings support past research indicative of dynamic triggering typically occurring in areas of pre-existing seismicity [Hill *et al.*, 1993; Anderson *et al.*, 1994; Husen *et al.*, 2004; Husker and Brodsky, 2004]. We infer triggered events found in the Coso region to be consistent with the “clock-advance” model [e.g., Gomberg, 2010, and references therein], the CGF displays a high susceptibility to remote triggering. We surmise, faults being triggered are already in a critical state and extremely close to failure, these triggered events are inevitable failures of the fault plane, activated prematurely due to the loading of imposed by dynamic stresses of the wavetrain of teleseismic events.

The majority of locations of locally triggered events reside either in the CGF or surrounding regional faults; consistent with previous observations indicating preferential triggering of geothermal areas and regions with pre-existing seismicity. We estimate PDS values ranging values ( $10^{-3}$ – $10^{-1}$  MPa), which is consistent with findings of Aiken and Peng (2014) indicating geothermal sites in California as susceptible to a triggering threshold of  $<0.001$  MPa.

We contribute to a growing body of observations that demonstrate that local seismicity can be triggered by the passage of seismic waves of large ( $M \geq 7$ ) earthquakes at remote distances upwards of 10,000 km away. To explain the triggering mechanisms in the case of instantaneous triggering in the CGF we propose direct failure of critically stressed faults by the Coulomb failure criteria [Kilb *et al.*, 2002; Hill, 2008]. However, the majority of locally triggered events occur after the passage of mainshock surface waves. Mechanisms to explaining this delay include: a change in frictional contact along a fault [Parsons, 2005], pore fluid diffusion [Brodsky and Prejean, 2005], and arrival of multiple surfaces circling the Earth [Peng *et al.*, 2011]. We propose a combination of these mechanisms incite a delay in the triggered response, although based on the properties of the CGF region, we surmise fluid diffusion to as the primary contributor in the development of the delay in triggered seismicity [e.g., Brodsky, 2006; Bodin and Gomberg, 1994; Syracuse *et al.*, 2010].

## References

- Anderson, J. G., J. N. Brune, J. N. Louie, Y. Zeng, M. Savage, G. Yu, Q. Chen, and D. dePolo (1994), Seismicity in the western Great Basin apparently triggered by the Landers, California, earthquake, 28 June 1992, *Bulletin of the Seismological Society of America*, 84(3), 863–891.
- Astiz, L. et al. (2014), The Array Network Facility Seismic Bulletin: Products and an Unbiased View of United States Seismicity, *Seismological Research Letters*, 85(3), 576–593, doi:10.1785/0220130141.
- Bodin, P., and J. Gomberg (1994), Triggered seismicity and deformation between the Landers, California, and Little Skull Mountain, Nevada, earthquakes, *Bulletin of the Seismological Society of America*, 84(3), 835–843.
- Boese, C. M., K. M. Jacobs, E. G. C. Smith, T. A. Stern, and J. Townend (2014), Background and delayed-triggered swarms in the central Southern Alps, South Island, New Zealand, *Geochem. Geophys. Res.*, 15(4), 945–964, doi:10.1002/2013GC005171.
- Brodsky, E. E. (2006), Long-range triggered earthquakes that continue after the wave train passes, *Geophys. Res. Lett.*, 33(15), L15313, doi:10.1029/2006GL026605.
- Brodsky, E. E., and S. G. Prejean (2005), New constraints on mechanisms of remotely triggered seismicity at Long Valley Caldera, *J. Geophys. Res.*, 110(B4), B04302, doi:10.1029/2004JB003211.
- Brodsky, E. E., V. Karakostas, and H. Kanamori (2000), A New Observation of Dynamically Triggered Regional Seismicity: Earthquakes in Greece Following the August, 1999 Izmit, Turkey Earthquake, *Geophysical Research Letters*, 27(17).
- Chao, K., Z. Peng, A. Fabian, and L. Ojha (2012), Comparisons of Triggered Tremor in California, *Bulletin of the Seismological Society of America*, 102(2), 900–908, doi:10.1785/0120110151.
- Chao, K., Z. Peng, H. Gonzalez-Huizar, C. Aiken, B. Enescu, H. Kao, A. A. Velasco, K. Obara, and T. Matsuzawa (2013), A Global Search for Triggered Tremor Following the 2011 Mw 9.0 Tohoku Earthquake, *Bulletin of the Seismological Society of America*, 103(2B), 1551–1571, doi:10.1785/0120120171.
- Crotwell, H. P., T. J. Owens, and J. Ritsema (1999), The TauP Toolkit: Flexible Seismic Travel-time and Ray-path Utilities, *Seismological Research Letters*, 70(2), 154–160, doi:10.1785/gssrl.70.2.154.
- Davatzes, N., and S. Hickman (2006), *Stress and faulting in the Coso Geothermal Field: Update and recent results from the East Flank and Coso Wash*, Proceedings 31st Workshop on Geothermal Reservoir Engineering, Stanford Univ., Stanford, CA.
- Duffield, W. A., C. R. Bacon, and G. B. Dalrymple (1980), Late Cenozoic volcanism, geochronology, and structure of the Coso Range, Inyo County, California, *J. Geophys. Res.*, 85(B5), 2381–2404, doi:10.1029/JB085iB05p02381.
- Van der Elst, N. J., H. M. Savage, K. M. Keranen, and G. A. Abers (2013), Enhanced Remote Earthquake Triggering at Fluid-Injection Sites in the Midwestern United States, *Science*, 341(6142), 164–167, doi:10.1126/science.1238948.
- Gomberg, J. (2010), Lessons from (triggered) tremor, *J. Geophys. Res.*, 115(B10), B10302, doi:10.1029/2009JB007011.
- Gomberg, J., and P. Johnson (2005), Seismology: Dynamic triggering of earthquakes, *Nature*, 437(7060), 830–830, doi:10.1038/437830a.

- Gomberg, J., P. A. Reasenberg, P. Bodin, and R. A. Harris (2001), Earthquake triggering by seismic waves following the Landers and Hector Mine earthquakes, *Nature*, *411*(6836), 462–466, doi:10.1038/35078053.
- Gomberg, J., P. Bodin, K. Larson, and H. Dragert (2004), Earthquake nucleation by transient deformations caused by the M = 7.9 Denali, Alaska, earthquake, *Nature*, *427*(6975), 621–624, doi:10.1038/nature02335.
- Gonzalez-Huizar, H., and A. A. Velasco (2011), Dynamic triggering: Stress modeling and a case study, *J. Geophys. Res.*, *116*(B2), B02304, doi:10.1029/2009JB007000.
- Gonzalez-Huizar, H., A. A. Velasco, Z. Peng, and R. R. Castro (2012), Remote triggered seismicity caused by the 2011, M9.0 Tohoku-Oki, Japan earthquake, *Geophys. Res. Lett.*, *39*(10), L10302, doi:10.1029/2012GL051015.
- Guilhem, A., Z. Peng, and R. M. Nadeau (2010), High-frequency identification of non-volcanic tremor triggered by regional earthquakes, *Geophys. Res. Lett.*, *37*(16), L16309, doi:10.1029/2010GL044660.
- Heidbach, O., M. Tingay, A. Barth, J. Reinecker, D. Kurfeß, and B. Müller (2010), Global crustal stress pattern based on the World Stress Map database release 2008, *Tectonophysics*, *482*(1–4), 3–15, doi:10.1016/j.tecto.2009.07.023.
- Hill, D. P. (2008), Dynamic Stresses, Coulomb Failure, and Remote Triggering, *Bulletin of the Seismological Society of America*, *98*(1), 66–92, doi:10.1785/0120070049.
- Hill, D. P., and S. G. Prejean (2014), Dynamic triggering, in *Treatise on Geophysics*, vol. 4, Elsevier, Amsterdam.
- Hill, D. P. et al. (1993), Seismicity Remotely Triggered by the Magnitude 7.3 Landers, California, Earthquake, *Science*, *260*(5114), 1617–1623, doi:10.1126/science.260.5114.1617.
- Husen, S., S. Wiemer, and R. B. Smith (2004), Remotely Triggered Seismicity in the Yellowstone National Park Region by the 2002 Mw 7.9 Denali Fault Earthquake, Alaska, *Bulletin of the Seismological Society of America*, *94*(6B), S317–S331, doi:10.1785/0120040617.
- Husker, A. L., and E. E. Brodsky (2004), Seismicity in Idaho and Montana Triggered by the Denali Fault Earthquake: A Window into the Geologic Context for Seismic Triggering, *Bulletin of the Seismological Society of America*, *94*(6B), S310–S316, doi:10.1785/0120040618.
- Hutton, K., J. Woessner, and E. Hauksson (2010), Earthquake Monitoring in Southern California for Seventy-Seven Years (1932–2008), *Bulletin of the Seismological Society of America*, *100*(2), 423–446, doi:10.1785/0120090130.
- Jagla, E. A. (2011), Delayed dynamic triggering of earthquakes: Evidence from a statistical model of seismicity, *EPL*, *93*(1), 19001, doi:10.1209/0295-5075/93/19001.
- Kilb, D., J. Gomberg, and P. Bodin (2000), Triggering of earthquake aftershocks by dynamic stresses, *Nature*, *408*(6812), 570–574, doi:10.1038/35046046.
- Kilb, D., J. Gomberg, and P. Bodin (2002), Aftershock triggering by complete Coulomb stress changes, *Journal of Geophysical Research B: Solid Earth*, *107*(4), 2–1.
- Miyazawa, M., E. E. Brodsky, and J. Mori (2008), Learning from dynamic triggering of low-frequency tremor in subduction zones, *Earth Planet Sp*, *60*(10), e17–e20, doi:10.1186/BF03352858.
- Morton, E. A., and S. L. Bilek (2014), Limited Dynamic Earthquake Triggering in the Socorro Magma Body Region, Rio Grande Rift, New Mexico, *Bulletin of the Seismological Society of America*, doi:10.1785/0120140021.

- Pankow, K. L. (2004), Triggered Seismicity in Utah from the 3 November 2002 Denali Fault Earthquake, *Bulletin of the Seismological Society of America*, 94(6B), S332–S347, doi:10.1785/0120040609.
- Parsons, T. (2005), A hypothesis for delayed dynamic earthquake triggering, *Geophysical Research Letters*, 32(4), doi:10.1029/2004GL021811.
- Parsons, T., and A. A. Velasco (2009), On near-source earthquake triggering, *J. Geophys. Res.*, 114(B10), B10307, doi:10.1029/2008JB006277.
- Parsons, T., and A. A. Velasco (2011), Absence of remotely triggered large earthquakes beyond the mainshock region, *Nature Geosci.*, 4(5), 312–316, doi:10.1038/ngeo1110.
- Parsons, T., J. O. Kaven, A. A. Velasco, and H. Gonzalez-Huizar (2012), Unraveling the apparent magnitude threshold of remote earthquake triggering using full wavefield surface wave simulation, *Geochem. Geophys. Geosyst.*, 13(6), Q06016, doi:10.1029/2012GC004164.
- Peng, Z., and K. Chao (2008), Non-volcanic tremor beneath the Central Range in Taiwan triggered by the 2001  $M_w$  7.8 Kunlun earthquake, *Geophysical Journal International*, 175(2), 825–829, doi:10.1111/j.1365-246X.2008.03886.x.
- Peng, Z., J. E. Vidale, A. G. Wech, R. M. Nadeau, and K. C. Creager (2009a), Remote triggering of tremor along the San Andreas Fault in central California, *J. Geophys. Res.*, 114(B7), B00A06, doi:10.1029/2008JB006049.
- Peng, Z., J. E. Vidale, A. G. Wech, R. M. Nadeau, and K. C. Creager (2009b), Remote triggering of tremor along the San Andreas Fault in central California, *J. Geophys. Res.*, 114(B7), B00A06, doi:10.1029/2008JB006049.
- Peng, Z., D. P. Hill, D. R. Shelly, and C. Aiken (2010), Remotely triggered microearthquakes and tremor in central California following the 2010  $M_w$  8.8 Chile earthquake, *Geophys. Res. Lett.*, 37(24), L24312, doi:10.1029/2010GL045462.
- Peng, Z., C. Wu, and C. Aiken (2011), Delayed triggering of microearthquakes by multiple surface waves circling the Earth, *Geophys. Res. Lett.*, 38(4), L04306, doi:10.1029/2010GL046373.
- Peng, Z., H. Gonzalez-Huizar, K. Chao, C. Aiken, B. Moreno, and G. Armstrong (2013), Tectonic Tremor beneath Cuba Triggered by the  $M_w$  8.8 Maule and  $M_w$  9.0 Tohoku-Oki Earthquakes, *Bulletin of the Seismological Society of America*, 103(1), 595–600, doi:10.1785/0120120253.
- Prejean, S. G., and D. P. Hill (2009), Earthquakes, Dynamic Triggering of, in *Encyclopedia of Complexity and Systems Science*, edited by R. A. M. Ph. D, pp. 2600–2621, Springer New York.
- Prejean, S. G., D. P. Hill, E. E. Brodsky, S. E. Hough, M. J. S. Johnston, S. D. Malone, D. H. Oppenheimer, A. M. Pitt, and K. B. Richards-Dinger (2004), Remotely Triggered Seismicity on the United States West Coast following the  $M_w$  7.9 Denali Fault Earthquake, *Bulletin of the Seismological Society of America*, 94(6B), S348–S359, doi:10.1785/0120040610.
- Roquemore, G. (1980), Structure, tectonics, and stress field of the Coso Range, Inyo County, California, *J. Geophys. Res.*, 85(B5), 2434–2440, doi:10.1029/JB085iB05p02434.
- Rubinstein, J. L., J. E. Vidale, J. Gomberg, P. Bodin, K. C. Creager, and S. D. Malone (2007), Non-volcanic tremor driven by large transient shear stresses, *Nature*, 448(7153), 579–582, doi:10.1038/nature06017.
- Syracuse, E. M., C. H. Thurber, C. J. Wolfe, P. G. Okubo, J. H. Foster, and B. A. Brooks (2010), High-resolution locations of triggered earthquakes and tomographic imaging of Kilauea Volcano's south flank, *J. Geophys. Res.*, 115(B10), B10310, doi:10.1029/2010JB007554.
- Tibi, R., D. A. Wiens, and H. Inoue (2003), Remote triggering of deep earthquakes in the 2002 Tonga sequences, *Nature*, 424(6951), 921–925, doi:10.1038/nature01903.



- Unruh, J. R., F. C. Monastero, and S. K. Pullammanappallil (2008), The Nascent Coso Metamorphic Core Complex, East-Central California: Brittle Upper Plate Structure Revealed by Reflection Seismic Data, *International Geology Review*, 50(3), 245–269, doi:10.2747/0020-6814.50.3.245.
- Velasco, A. A., S. Hernandez, T. Parsons, and K. Pankow (2008), Global ubiquity of dynamic earthquake triggering, *Nature Geosci*, 1(6), 375–379, doi:10.1038/ngeo204.
- Velasco, A. A., R. A. Alfaro-Diaz, D. Kilb, and K. Pankow (2015), A Time-Domain Detection Approach to Identify Small Earthquakes within the Continental U.S. Recorded by the USArray and Regional Networks, *In Prep*.
- West, M., J. J. Sánchez, and S. R. McNutt (2005), Periodically Triggered Seismicity at Mount Wrangell, Alaska, After the Sumatra Earthquake, *Science*, 308(5725), 1144–1146, doi:10.1126/science.1112462.

## Vita

Richard Alexander Alfaro-Diaz was born in San Juan, Puerto Rico. The son of Ricardo L. Alfaro and Linda Diaz-Howard, he graduated from Montwood High School in 2009 and enrolled at the University of Texas at El Paso (UTEP). While pursuing a Bachelor of Science degree in Geological Sciences, he conducted undergraduate research as a Keck Geology Consortium Project Fellow in 2013. He completed an Undergraduate Thesis on a study of the “Activation of a Secondary Oblique Slip Fault Following the Mw=7.6 Sept 5, 2012, Nicoya Costa Rica, Earthquake” the results of which were published as a Keck Short Contribution. He was a volunteer tutor for Ysleta High-school in the Ysleta Independent School District from 2009-2013. Mr. Alfaro was a Member of the Society of Collegiate Scholars from 2010-2015, and the treasurer for the UTEP-SACNAS chapter from 2013-2014. He received undergraduate scholarships and awards including the, W.P. Nash Scholarship, Africa Array Scholarship in 2013, a Keck Geology Consortium Fellowship in 2013, qualified for the Dean’s list Spring/Fall 2010, Spring 2011, Spring/Fall 2012, Fall 2013 and received an undergraduate award for Research Excellence in 2013. He graduated with honors *cum laude* from UTEP in the fall of 2013. Mr. Alfaro then enrolled in the Masters of Geophysics program at UTEP in the spring of 2013. While a graduate student, he worked as a research assistant in 2014. He then received a National Science Foundation scholarship; from the program Student Mentoring to Achieve retention: Triads in Science (SMARTS) from 2014-2015. Through the SMARTS program he mentored an undergraduate student in the geology department to ensure engagement, and success in their undergraduate research. Mr. Alfaro received the Science, Technology, Engineering and Math education (STEM) GK-12 Graduate Fellowship from 2014-2015. As an NSF GK-12 fellow Mr. Alfaro participated as a “Scientist in Residence” at the Valle Verde Early College High

School campus and in conjunction with UTEP faculty, Taught, created labs, and gave lectures on research. He related geological and geophysical concepts to high school Physics. He also participated in 2014 International American Geophysical Union meeting, presenting as a first author. Mr. Alfaro received a marathon oil scholarship in 201, and actively participated as a member of UTEP's Society of Exploration Geophysicists (2014-2015).

Permanent address: 11308 Lake Ozarks  
El Paso, Texas, 79936

This thesis was typed by Richard A. Alfaro-Diaz